Solar Energy Materials & Solar Cells 307 (2026) 114608

Contents lists available at ScienceDirect

Solar Energy Materials and Solar Cells

journal homepage: www.elsevier.com/locate/solmat

End-of-life management of crystalline silicon photovoltaic modules: current technologies, economic constraints and future perspectives

Andrea Franzoni [a,*], Mariasole Bannò [a], Mattia Avanzini [b]

[a] Department of Mechanical and Industrial Engineering, University of Brescia, Via Branze 38, Brescia, 25123, Italy
[b] A2A S.p.A., Via Lamarmora 230, Brescia, 25124, Italy

ARTICLE INFO

Keywords:
End-of-life management
Photovoltaic module
Recycling
Review
Sustainability transition

ABSTRACT

The energy transition towards net-zero emissions is accelerating the global spread of photovoltaics (PV), simultaneously generating a growing flow of end-of-life (EoL) modules whose management represents one of the most urgent environmental and economic challenges in the sector. Crystalline silicon (c-Si) modules, which dominate the market with a share exceeding 90 %, will constitute the main component of this waste stream, with cumulative volumes estimated between 60 and 78 million tonnes by 2050. Despite the growing interest from the scientific community, most of the proposed recycling technologies remain in the experimental phase, and critical aspects such as process costs, the quality of recovered materials, and the generation of secondary pollutants are still insufficiently addressed. This review critically analyses delamination and material recovery technologies for EoL c-Si modules, discussing their strengths, limitations, and development prospects, with particular attention to the technical, economic and environmental conditions necessary for the transition to industrially mature processes. The objective is to provide an updated analytical framework that can guide research and development choices in a sector poised for rapid growth in the coming decades.

1. Introduction

The global energy transition requires a rapid and widespread adoption of renewable sources, in line with international commitments to reduce greenhouse gas emissions. In Europe, the Green Deal aims to reduce greenhouse gas emissions by at least 55 % by 2030 compared to 1990 levels, while simultaneously increasing the share of energy from renewable sources to 40–45 % [1,2]. In this scenario, PV technology plays a leading role. In 2022, it contributed to 4 % of global electricity production, with projections indicating an installed capacity exceeding 14 TW by 2050, when it could meet about one-third of the world's energy needs [1,3–5]. PV technology stands out for its ability to generate electricity without direct emissions of pollutants, with the possibility of being installed on very different scales, from small domestic systems to large solar parks, characteristics that make it the renewable source with the highest potential for replacing fossil fuels [6].

Since their commercial introduction, PV modules have undergone significant technological evolution, characterised by a constant increase in conversion efficiency and a gradual reduction in production costs [4,7]. Such development has favoured widespread adoption globally; however, research has predominantly focused on optimising operational performance and module lifespan, neglecting aspects related to their EoL management. Although the first studies on solar cell recycling date back to the early 2000s, the development of effective recovery strategies has received relatively limited attention compared to the effort devoted to performance improvement. This imbalance has resulted in a delay in the development of mature recycling technologies, which are increasingly urgent in light of the growing volume of PV waste expected in the coming decades [8,9].

The expansion of the market, while essential for achieving decarbonisation goals, also introduces a new and pressing environmental and economic challenge, namely the management of EoL modules. The first installed systems are already reaching the end of their useful life, conventionally estimated at 25–30 years, corresponding to the moment when the nominal power drops to 80 % of the initial value [5,10–12], and will contribute in the coming decades to generating enormous volumes of waste. Projections from the International Renewable Energy Agency (IRENA) indicate that between 1.7 and 8 million tonnes of modules will become waste by 2030, with an expected increase to 60–78 million tonnes by 2050 [13]. The heterogeneous composition of the

This article is part of a special issue entitled: Recycling of PV modules published in Solar Energy Materials and Solar Cells.

* Corresponding author.
E-mail address: andrea.franzoni@unibs.it (A. Franzoni).

https://doi.org/10.1016/j.solmat.2026.114608
Received 30 April 2026; Received in revised form 6 July 2026; Accepted 28 July 2026
Available online 31 July 2026

modules, which includes tempered glass, encapsulating polymers, silicon, and metals, necessitates the development of dedicated treatment and recovery processes. The European Union has recognised the significance of this waste stream by including EoL PV modules in the category of waste from electrical and electronic equipment (WEEE) since 2012 [14,15]. However, at the global level, the regulatory framework remains fragmented and often insufficient, while recycling infrastructures are still inadequate to handle the expected volumes [1,8,16].

The recycling of PV modules gains importance not only from an environmental perspective but also from an economic and geopolitical standpoint. The growing demand for raw materials in the PV industry, particularly silicon, silver, and copper, has made the vulnerability of global supply chains evident. The European Union has included silicon among the critical raw materials for the energy transition, emphasising the need for recovery strategies to reduce dependence on imports and increase industrial resilience [9,17]. The efficient recovery of valuable materials from EoL modules thus represents both an environmentally sustainable solution and a measure of economic and industrial security.

PV market is currently dominated by crystalline silicon (c-Si) modules, in both monocrystalline and polycrystalline variants, which represent between 90 % and 95 % of all global installations and will proportionally constitute the most significant share of the sector's waste stream in the coming decades [4,15,16,18,19]. Alternative technologies, such as thin-film modules (CdTe, CIGS, a-Si) and emerging third-generation solutions (organic cells, perovskites, dye-sensitized cells), still occupy a marginal share of the market and, despite presenting interesting development prospects, will not contribute substantially to the waste volume in the short and medium term [20,21].

Despite the recognised necessity and potential value of recycling, only an estimated share of around 10 % of decommissioned PV modules is actually recycled globally [17,22]. The remaining modules are, for the most part, landfilled or disposed of together with general and electronic waste, while a smaller and poorly quantified fraction is reused on second-hand markets, although reliable global figures on their fate are scarce [13]. The main reasons for this delay lie in the technological complexity of the delamination and material separation processes, the low economic profitability of existing recovery chains, which often limit themselves to the recovery of aluminium, glass, and copper, neglecting high-value materials such as silicon and silver, and the lack of a stable and sufficient waste stream to support the initiation and continuity of dedicated industrial plants [9,23]. This is compounded by the fact that the actual lifespan of the panels has proven to be longer than initial estimates, with an efficiency degradation rate of around 0.5 % per year instead of the expected 1 %, which has delayed the emergence of the waste stream and disincentivised investments in the sector [9].

Research on c-Si PV module recycling is evolving rapidly, and a large share of the literature analysed in this review was published between 2023 and 2025, which makes a continuously updated and critical synthesis necessary. Recent reviews have addressed the topic from complementary angles, focusing on the technical assessment of recycling processes and the identification of research gaps [24], on hydrometallurgical routes for the recovery of critical and high-value materials [25], or on policy-oriented recommendations such as extended producer responsibility and economic incentives [26]. Building on these contributions, the aim of this review is to provide an updated and critical analytical framework on the recycling of EoL c-Si PV modules. To this end, the specific objectives are: (i) to describe the structure and material composition of c-Si modules relevant to their recyclability; (ii) to review and critically compare the available delamination technologies; (iii) to analyse the processes for the recovery and purification of the main material fractions (glass, silicon, silver, aluminium, copper, tin and lead); (iv) to review the environmental performance of the recycling routes through life cycle assessment; (v) to assess the economic sustainability of recycling and the technical-economic conditions required for industrial-scale implementation; and (vi) to identify the main limitations, the generation of secondary pollutants and the priorities for future research and development. In this way, the review intends to support research, development and investment decisions in a sector poised for rapid growth.

2. Methodology

A structured literature search was carried out on the Scopus and Web of Science databases, applied to title, abstract and keywords. The search combined terms covering three domains, namely the photovoltaic field, the module or panel as the object of treatment, and the recovery, recycling and reuse of its materials. The search returned 491 records in Scopus and 422 in Web of Science. Results were restricted to journal articles, written in English and in the final publication stage, and, after combining the two databases and removing 266 duplicates, 354 records were screened by title and abstract. Of these, 96 were assessed in full text and 70 met the inclusion criteria and were included in the review of recycling and recovery technologies. Studies were considered eligible if they addressed the recovery or recycling of materials from crystalline silicon photovoltaic modules, covering either the entire treatment chain or a specific stage of it. The identification and selection process is summarised in the flow diagram of Fig. 1.

3. c-Si PV module structure and composition

This review focuses on c-Si PV modules, which represent over 90 % of the global market and will continue to constitute nearly all of the waste stream in the medium term [4,15,16,18,27]. Although the basic structure of these modules has remained largely unchanged over the past forty years, technological evolution has led to significant variations in material composition and production techniques [28].

A c-Si module is a laminated structure device composed of multiple overlapping functional layers bonded together through high-temperature lamination processes (Fig. 2a). The typical configuration includes: a front layer of high-transparency tempered glass, which ensures mechanical protection and maximum optical transmission to the cells; two layers of encapsulant material in ethylene-vinyl acetate (EVA), one front and one rear, that envelop the PV cells protecting them from thermal, mechanical, and moisture agents; the c-Si cells with their respective metal contacts; a multilayer polymeric backsheet on the rear side; a perimeter frame in aluminium that provides structural stability and facilitates installation; and a junction box applied on the back for electrical connection with the system [1,29].

The laminated structure of the module, while ensuring mechanical robustness and operational durability, represents the main challenge in recycling processes, as the separation of individual layers requires specific thermal, chemical, or mechanical treatments.

EVA represents the most widely used encapsulation material in the sector, with a market share that reached approximately 90 % in 2019 [30,31]. Its widespread use is due to its excellent adhesive properties, high optical transparency, good thermal stability, and low production cost [30]. The average thickness of each EVA layer generally varies between 300 and 450 μm, contributing approximately 5–7 % by weight to the module [5]. During the lamination phase, EVA is cross-linked using chemical agents, acquiring a three-dimensional structure that ensures its mechanical and adhesive properties over the long term. This cross-linking makes its decomposition one of the most critical aspects of recycling. The breaking of cross-linked bonds indeed requires high temperatures in pyrolysis processes, or the use of specific organic solvents in chemical approaches, with significant implications in terms of energy costs and by-product management. The polymeric backsheet serves as an electrical and mechanical barrier. The most common types are three-layer composite structures, mainly classified into: TPT (Tedlar®/PET/Tedlar®), based on polyvinyl fluoride (PVF); KPK (Kynar®/PET/Kynar®), based on polyvinylidene fluoride (PVDF); and PPE (PET/PET/EVA), free of fluoropolymers [1,30]. The presence of

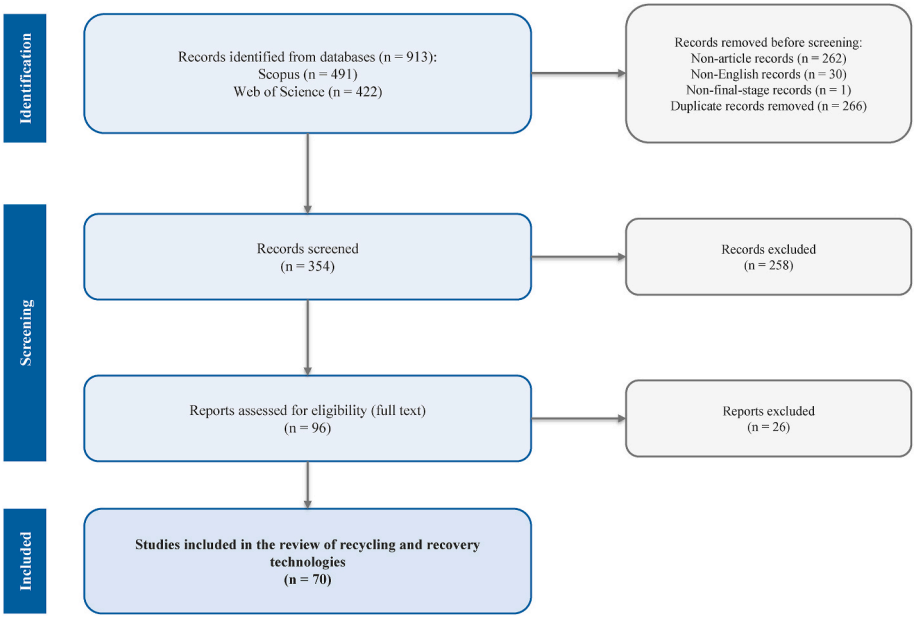

Fig. 1. Flow diagram of the identification and selection of the studies included in the review of recycling and recovery technologies.

fluoropolymers in the backsheet constitutes a significant concern in thermal processes, as their decomposition generates gaseous by-products containing fluorine that require specific abatement and treatment systems.

The PV cell is the active component of the module and has a multi-layer structure (Fig. 2b). The substrate consists of an ultra-pure silicon wafer, doped with boron or phosphorus to form the p-n junction that generates the potential difference at the base of the PV conversion. The thickness of the wafer has progressively decreased over the years, going from over 300 μm in older technologies to less than 180 μm in next-generation cells [16,28].

On the front side of the cell, an anti-reflective coating (ARC) made of silicon nitride is deposited, which reduces optical losses due to reflection and improves conversion efficiency. The front electrical contacts are made using a screen-printed and sintered silver grid on the surface, while the rear contact typically consists of a continuous layer of aluminium [5,30].

The cells are interconnected by tinned copper ribbons that collect and transmit the generated current to the junction box [5,29]. The average mass composition of a c-Si module is characterised by the predominance of glass, followed by polymers, the aluminium frame, and the silicon of the cells [5,20,32]. Table 1 summarises the average composition of a c-Si module.

Despite the overall composition remaining structurally similar over time, there is significant variability among manufacturers, years of production, and technological generations. These differences, related to the type of backsheet, the formulations of the polymers, and the concentration of metals in the electrical contacts, directly influence the efficiency of recycling processes and the possibility of standardising recovery techniques [28,33]. The increasing heterogeneity of materials, while improving the operational performance of modules, complicates EoL management and requires a flexible approach in the choice of treatment technologies.

From an economic and strategic perspective, silicon and silver represent the most interesting materials, although they are present in different proportions. The silicon wafer accounts for over 50–60 % of the total cost of the cell and requires high purity levels, at least 6N for PV applications, whose production is an energy-intensive process [17, 33–35]. Silver, despite representing less than 0.1 % by weight of the module with a concentration of about 600–630 g per tonne [20,36], constitutes up to 35 % of the overall economic value derived from recycling due to its high market price [20,27,36]. Copper, present in ribbons and wiring, contributes approximately 5 % of the total recoverable value [37]. On the contrary, polymeric materials such as EVA and backsheet, despite representing a significant fraction of the module's mass, have low market value and are difficult to process, constituting one of the main technological barriers to complete and economically sustainable recycling [5]. The presence of heavy metals such as lead and tin, even if in limited quantities, necessitates the adoption of safe treatment techniques to avoid environmental contamination risks [6, 32].

4. Disassembly and delamination processes of c-Si PV modules

The recycling of EoL c-Si PV modules is a process articulated in multiple phases, which begins before any material recovery operations. The complexity of the module's laminated structure prevents direct access to valuable materials without a preliminary sequence of separation and delamination operations [5,38,39]. The recycling of a c-Si module can be described through three successive phases: the mechanical disassembly of peripheral components, the delamination of the laminated structure to separate its constituent layers, and the recovery and purification of target materials [3,5].

The efficiency of the preliminary stages is a determining factor for the overall performance of the recycling process, as the degree of separation achieved in this phase directly affects the purity and recovery yield of all materials extracted in the subsequent stages [5]. In particular, the removal of the EVA encapsulant represents the central technical challenge of the entire pre-treatment sequence [37,39]. The choice of delamination strategy has profound implications not only on the efficiency of the process but also on the integrity of the recovered materials, the generation of secondary pollutants, and the economic feasibility of the recycling chain [8,12].

As illustrated in Fig. 3, the pre-treatment of c-Si modules can be organised into two sequential phases: an initial disassembly phase, in which the aluminium frame and junction box are removed from the module, followed by a delamination phase, in which the laminated core is treated to separate glass, cells, backsheet, and encapsulant. Delamination technologies are classified into four categories: mechanical, thermal, chemical, and advanced delamination. The first three categories group methods that operate predominantly through a single principle of action. The fourth category, called “advanced processes,”

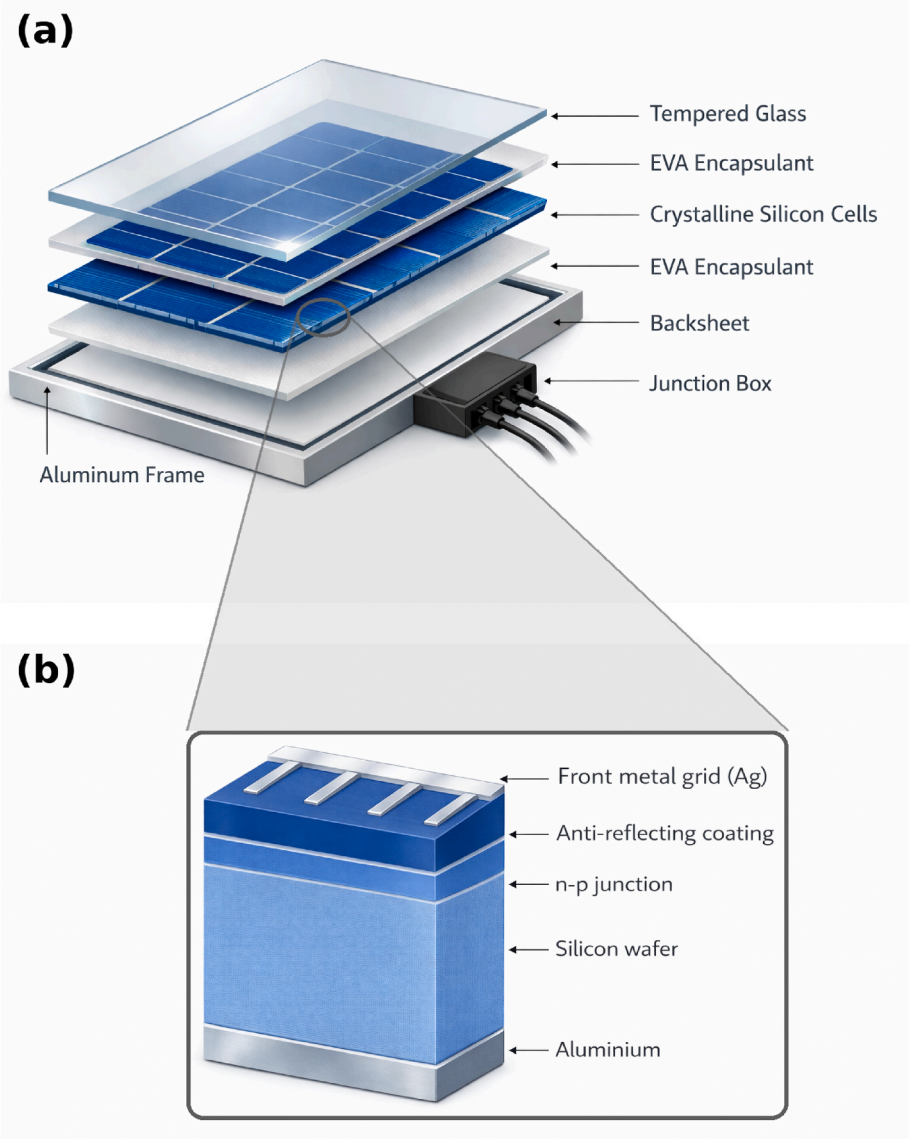

Fig. 2. (a) Crystalline silicon photovoltaic module structure; (b) crystalline silicon solar cell structure, corresponding to a magnification of the cell within the module stack shown in (a). (For interpretation of the references to colour in this figure legend, the reader is referred to the Web version of this article.)

Table 1
Mass percentage composition of a typical c-Si PV module [5,24,26].

Component	Main materials	%
Front glass	Temper glass	70–76
Frame	Aluminium	8–10
Encapsulant (Front + Back)	EVA	5–7
Backsheet	PET/fluoropolymers	2–4
Silicon wafer	Silicon	3–5
Front conductor	Silver	<0.1
Back conductor	Aluminium	0.5–1
Ribbon/Cables	Copper	~1
Solder	Tin, lead	<0.1
Junction Box	polymers, copper	~1–2

encompasses technologies characterised by an intrinsically higher technological complexity, arising from the need to simultaneously control multiple operational variables of a physical, thermal, and chemical nature. It is important to clarify that this designation does not imply a higher technological maturity but rather reflects the technological sophistication required for their implementation.

4.1. *Disassembly: removal of the aluminium frame and the junction box*

Before any delamination treatment, PV modules undergo a disassembly operation aimed at removing peripheral components that are not part of the laminated structure, namely the aluminium frame and the junction box. This preliminary operation is justified by both technical and economic considerations. The aluminium frame, which typically represents 8–10 % of the module's mass, is a high-value material that can be recovered with high purity through simple mechanical operations; its preventive removal also simplifies subsequent delamination treatments, reducing the overall size and rigidity of the module [12]. Similarly, the junction box and copper cables, although representing a smaller fraction of the total mass, contain recoverable copper separately with minimal processing effort [5,29].

Disassembly can be performed manually or using automated mechanical systems. Manual disassembly is the most reported approach in laboratory-scale studies, where operators remove the frame by unscrewing or cutting the fastening clips and detach the junction box by severing the cables at the entry point. Although it is a simple and non-destructive method for the laminated core of the module, manual disassembly is labour-intensive and poorly suited for industrial-scale

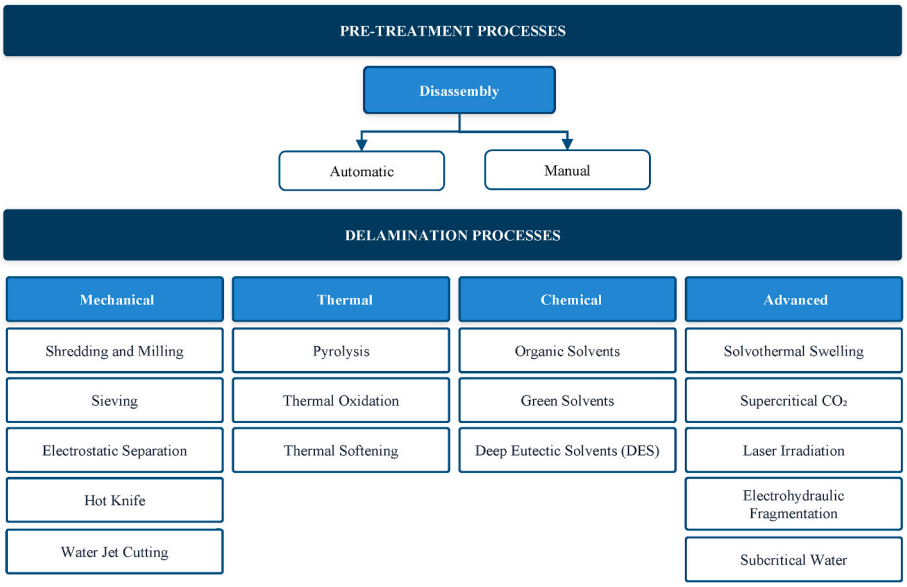

Fig. 3. Sequence of pre-treatment processes.

operations. Automated disassembly systems, based on robotic arms, hydraulic presses, pneumatic clamps, or dedicated cutting tools, have been developed to operate with high precision, ensuring the separation of the frame without causing damage to the tempered glass [24]. The residual laminated module, composed of tempered glass, front EVA, silicon cells, rear EVA, and backsheet, then proceeds to the delamination phase.

4.2. Thermal delamination

Thermal delamination exploits the action of heat to modify the physical properties or induce the thermochemical decomposition of the polymeric components of the module, releasing the layers (glass, cells, metal contacts) from the laminate. It is one of the most widely studied approaches in the literature and is generally considered to have the highest potential for industrial implementation, particularly in its pyrolytic variant, due to relatively short process times, high polymer removal efficiency, and the absence of liquid chemical reagents [8,11]. According to the operating conditions adopted and the treatment objective, the thermal processes applied to the delamination of c-Si modules can be classified into three main subcategories: pyrolysis in an inert atmosphere, controlled thermal oxidation in an oxidising atmosphere, and low-temperature heating for EVA softening without decomposition.

Pyrolysis in an inert atmosphere - Pyrolysis is the most studied thermal process for the delamination of c-Si modules. It consists of heating the module in the absence of oxygen, typically in a nitrogen atmosphere, at temperatures sufficient to thermochemically decompose the present polymers, converting them into gaseous and liquid products, while the inorganic components remain substantially unchanged [11]. The thermal decomposition of EVA follows a two-stage mechanism: in the first stage, between approximately 300 and 410 °C, the acetate groups undergo a deacetylation reaction with the release of acetic acid as a gaseous byproduct; in a second stage, above 410 °C, the main polyethylene chain undergoes cleavage, forming alkenes, alkadienes, and cyclic compounds [40,41]. The complete removal of EVA is typically achieved at temperatures between 480 and 600 °C, with treatment durations ranging from 7 to 90 min depending on the specific operating conditions [28,40–42]. Numerous studies in the literature converge in indicating that pyrolysis at 500 °C in a nitrogen atmosphere represents an effective benchmark for the complete removal of module polymers [28,41,43].

A critical aspect of pyrolysis is the presence of the fluoropolymer-based backsheet. Its thermal decomposition generates toxic gaseous byproducts, particularly hydrogen fluoride (HF), fluoroalkanes, and aromatic compounds, which require dedicated abatement systems and significantly increase the costs and environmental impact of the process [28,41]. To address this issue, several authors have proposed the preventive removal of the backsheet prior to pyrolytic treatment. Camargo et al. demonstrated that the mechanical removal of the backsheet using a rotary milling tool before pyrolysis significantly reduces the generation of fluorinated by-products and shortens the time required for subsequent delamination stages by over 45 %, achieving complete polymer removal after 20 min at 500 °C [2]. Life Cycle Assessment studies suggest that pyrolytic treatment can have a competitive or lower environmental impact compared to other c-Si module recycling technologies under specific operating conditions, making it one of the promising options for the industrial development of the sector [21].

An alternative method for reducing the generation of fluorinated by-products is the two-stage pyrolysis process, which involves an initial low-temperature heating for the mechanical removal of the backsheet, followed by a second high-temperature stage for the complete decomposition of EVA. Wang et al. proposed two-stage protocols in which the module is first heated to 150 °C for 5 min, bringing the EVA to a degree of softening that allows for the manual or mechanical removal of the backsheet, followed by a second stage at 500 °C for the complete decomposition of the residual EVA, with over 99 % by weight of the polymers removed [43]. This strategy avoids the co-pyrolysis of the fluorinated backsheet with EVA, eliminating the main source of HF emissions.

Thermal oxidation - As an alternative to pyrolysis in an inert atmosphere, some studies have investigated thermal treatment in the presence of controlled amounts of oxygen or air. Unlike traditional pyrolysis, controlled thermal oxidation exploits the partial combustion of the organic fraction to promote a more complete decomposition of EVA, minimising the formation of carbonaceous residues on the recovered materials. Fiandra et al. proposed a two-stage process in which the module is first subjected to the mechanical removal of the fluorinated backsheet using a milling machine, followed by a thermal treatment in an oxidising atmosphere at 500 °C for 1 h, achieving the complete degradation of the residual EVA with only traces of carbon on the recovered materials and an overall recovery of approximately 90 % of the total module weight [44]. Camargo et al. confirmed the effectiveness of controlled thermal oxidation at 500 °C for 90 min, achieving complete

degradation of the polymers and a metal concentration approximately 20 times higher than the starting material [42].

Thermal softening - A third subcategory of thermal processes does not directly aim at the decomposition of polymers, but rather at their simple softening through moderate temperatures to reduce adhesion between layers and facilitate their mechanical separation. These approaches operate at temperatures typically ranging from 90 to 200 °C and are often employed as the first stage of a two-stage process or as a stand-alone method for backsheet removal. Riech et al. used a quartz halogen lamp to heat the module to 90–120 °C, softening the EVA and allowing for the mechanical removal of the backsheet before a subsequent thermal treatment at 600 °C for 30 min for the complete combustion of the EVA [7]. Dobra et al. proposed a protocol in which the module is heated in a muffle furnace at 170 °C for 10 min, followed by thermal treatment at 600 °C for 18 min for the complete removal of polymers [28]. Królikowski et al. demonstrated that by heating the module to 130 °C on a heating plate, it is possible to separate the backsheet and subsequently raising it to 170 °C allows for the mechanical removal of the glass [45].

It is worth noting the study by Wu et al., which introduced a variant that combines a low-temperature treatment of −40 °C for 3 min, which embrittles the back EVA and facilitates the mechanical detachment of the backsheet, with subsequent pyrolysis at 650 °C for 30 min, achieving complete delamination with the possibility of recovering the intact backsheet [46].

Despite its overall advantages, thermal delamination presents limitations that must be carefully managed on an industrial scale. The high energy consumption associated with high process temperatures, particularly in the pyrolytic variant, represents a significant cost factor and a source of greenhouse gas emissions. The gaseous byproducts of EVA and backsheet decomposition require effective treatment systems. Moreover, the mechanical stresses induced by the different thermal expansion of the module layers and the pressure of the gases generated during the decomposition of the front EVA can cause the fracture of the silicon cells during treatment, a problem particularly relevant for next-generation cells with a thickness of less than 180 μm, reducing the integrity of the recovered wafers [24,26].

4.3. Mechanical delamination

Mechanical delamination includes processes that achieve the separation of layers through the application of macroscopic compressive, shear, or impact forces, without the use of chemical reagents, high process temperatures, or advanced energy technologies. These methods are characterised by low energy consumption, relatively simple equipment, and the absence of gaseous or liquid by-products that require dedicated treatments [12]. However, conventional mechanical delamination does not allow for the complete dissolution or decomposition of EVA, and the recovered fractions typically contain polymeric residues that require further treatments [21,26].

Shredding, grinding, and sieving - The most widely studied mechanical approach is size reduction through shredding or milling, in which the module is crushed into granular material using hammer mills, blade mills, rotary crushers, or multi-stage combinations of these. After size reduction, the resulting mixture of glass, silicon, metals, and polymer fragments is usually subjected to screening, which separates the material into fractions of different particle sizes. Due to the different mechanical properties and densities of the constituent materials, each fraction tends to be enriched with specific components: the coarser fractions (>4–8 mm) typically retain a greater proportion of EVA and backsheet fragments, the intermediate fractions (1–5 mm) are enriched in glass, and the finer fractions (<0.5–1 mm) concentrate the metallic components and silicon particles [15,23,40].

Several studies have detailed the particle size distribution of the crushing products. Salazar et al. used a blade mill for 15 min at 400 W in two successive stages to obtain particles with a size <6.35 mm, followed by sieving into three categories: the fraction >4 mm containing 33.71 % of polymers, the fraction 0.5–2 mm with 99.37 % of copper and 76.85 % of total glass, while the fraction <0.25 mm containing 94.12 % of the total silver in the module [47]. The purity of the fractions recovered using conventional mechanical methods is, however, limited by the residual presence of polymers and cross-contamination between materials, and additional separation or treatment stages are generally required to obtain materials suitable for secondary reuse [47].

Dias et al. employed a blade mill followed by sieving into three fractions (<0.5 mm, between 0.5 mm and 1 mm, and >1 mm), demonstrating that subsequent pyrolysis at 500 °C for 30 min in an inert atmosphere allows for the removal of 99 % of the polymers present in the granular fractions [40].

To improve the efficiency of mechanical separation and reduce the amount of material requiring subsequent treatments, some authors have proposed multi-stage approaches that combine crushing with integrated physical separation operations. After the removal of the aluminium frame Azeumo et al. subjected the modules to crushing with a blade mill, followed by heavy medium separation, further grinding, and sieving, obtaining approximately 76 % glass with a purity of about 100 % and 100 % of metals with a purity of 67 % [48]. Physical separation based on sieving has intrinsic limitations related to the difficulty of effectively separating fine fractions and the not always sufficient purity of the obtained products, typically requiring integration with complementary separation techniques such as electrostatic or fluidised bed separation, discussed in the following paragraphs [20,27].

Size-based separation - Whereas sieving was introduced above simply as a way to split the crushed material, size-based separation uses the same screening principle in a targeted way, to pre-concentrate the valuable fine fractions before the chemical recovery. After comminution, the crushed material is fractionated by particle size using vibrating screens or sieves with different mesh openings. The module components report to different size classes, so that the silver concentrates in the smallest fractions, where about 80 % of it is found [11], together with the fine silicon particles, whereas the polymeric fragments from EVA and backsheet remain mostly in the coarser fractions [49]. Size-based separation therefore acts as a low-cost pre-concentration step that improves the efficiency of the downstream chemical recovery [11].

Magnetic separation - Beyond sorting by size, the crushed stream can also be separated according to the magnetic behaviour of its components. Once the material is crushed and screened, a magnetic separator removes any ferromagnetic particles from the stream; in a c-Si module, however, this fraction is very small, since the main metals (silver, aluminium, copper and tin) are not ferromagnetic and the frame and junction box are removed beforehand during disassembly, so magnetic separation is of limited relevance [50]. More useful is eddy-current separation, in which a time-varying magnetic field induces currents in the conductive particles and deflects the non-ferrous metals, such as aluminium, away from the non-metallic fraction [51]. Like the other mechanical techniques these methods are reagent-free and operate at room temperature, but they provide only a coarse separation that usually requires subsequent refining.

Electrostatic separation - Electrostatic separation has been proposed as a complementary technique to improve the separation of conductive fractions from non-conductive ones after mechanical crushing. By passing the ground material through a high-voltage electrostatic field generated by a rotating roller separator, conductors (metals, silicon), semiconductors, and non-conductors (glass, polymers) are deflected towards different collection zones based on their surface charge behaviour [20,27,32]. Dias et al. subjected the modules to mechanical grinding to sizes smaller than 2 mm and subsequent electrostatic separation with a field of 24 kV and a rotation speed of 30 rpm, achieving separation into conductive and non-conductive fractions and concentrating over 90 % of the total metals in the conductive fraction, providing a suitable starting material for subsequent hydrometallurgical treatment [27]. Despite the relative simplicity and low environmental impact of the process, electrostatic separation shows significant

limitations in managing fine fractions and in the selective separation between different metals. Li et al. applied electrostatic separation specifically for the recovery of silicon from fine fractions, using a rotating roller separator operating at 15 kV on crushed material with a particle size between 0.3 mm and 0.45 mm, achieving silicon with 91 % purity [32].

Hot knife - The hot knife method involves passing a heated blade or wire through the EVA layer between the glass and the solar cells, softening the encapsulant locally and allowing the glass sheet to be separated cleanly from the rest of the module. The method allows for rapid and non-destructive removal of the glass while preserving the integrity of the underlying cell structure [26,52]. The technique separates the front glass from the backsheet-side laminate of standard glass-backsheet modules, using a blade heated to about 180 to 200 °C [53]. Each module is processed in about 50 s, and the process requires flat, undamaged modules, being unable to treat units with bent frames or broken glass [54]. Its application as a preliminary phase was reported by Takaya et al., where the hot knife is used for the removal of the glass layer before subsequent treatment with electric pulses for the exposure and recovery of silver wires from still-encapsulated photovoltaic cells [55].

Water jet cutting – Water jet cutting shares with the hot-knife method the aim of recovering the tempered glass without breaking it, but it relies on the mechanical erosion produced by a pressurised water jet instead of a heated blade. A high-pressure water jet, sometimes combined with an abrasive, scrapes away the silicon layers together with the EVA encapsulant while leaving the module glass intact and clean, so that the glass can be recovered without breakage and without chemical reagents or high temperatures. On c-Si modules the technique is used mainly to separate and reclaim the tempered glass, because damaging the glass would make its recycling more energy-intensive than the energy saved by recovering it; the separated glass is clean and free of harmful residues and needs no further treatment for EVA removal, while the wastewater generated is managed through dedicated filtration [50]. Reported industrial systems rely on robotic or CNC water-jet machines, with an energy consumption of about 20 kW for glass separation [50]. The fragmented mixture of solar cells and EVA is then sent to subsequent sorting and extraction steps for material recovery.

4.4. Chemical delamination

Chemical delamination is based on the use of liquid solvents or chemical agents that dissolve, swell, or depolymerise the EVA encapsulant, interrupting its adhesion to adjacent layers and allowing for separation. The dissolution of EVA in organic solvents follows the standard polymer dissolution model, where solvent molecules diffuse into the polymer matrix causing plasticization and progressive swelling of the material until the adhesive bonds break [56]. EVA consists of a crosslinked portion and a non-crosslinked portion: organic solvents predominantly dissolve the non-crosslinked part, while inducing swelling in the crosslinked part, resulting in an increase in resin volume that reduces adhesion between layers [21]. Chemical approaches operate at relatively low temperatures and do not generate pyrolysis gases, making them particularly interesting for the recovery of intact high-quality glass sheets and undamaged silicon wafers. However, the use of chemical reagents introduces concerns related to solvent toxicity, reagent consumption, liquid waste management, and process costs, which represent the main barriers to industrial implementation [9,23].

Traditional organic solvents – Among the most studied agents for chemical delamination are chlorinated organic solvents, particularly trichloroethylene (TCE) and dichlorobenzene. Doi et al. demonstrated that immersion in TCE at 80 °C for 10 days allows for the complete dissolution of EVA and the recovery of intact silicon cells without damage, establishing proof of concept for chemical delamination [34]. Subsequent studies have confirmed the effectiveness of TCE and other chlorinated solvents (toluene, o-dichlorobenzene), but have also highlighted significant challenges [18,34,35,39,57,58]. Prasad et al. optimised the process with TCE at 70 °C for 8 h, achieving an effective separation of the module layers from EVA [35]. Brenes et al. adopted a combination of toluene and distilled water at 80 °C for 120 min, achieving the removal of 72 % of EVA, with the residue eliminated through subsequent calcination at 500 °C [59]; Chitra et al. instead used pure toluene at 50 °C with mechanical agitation at 600 rpm for 3 days, demonstrating the possibility of recovering and reusing the solvent through chemical distillation [57]. Vaňek et al. reported the complete separation of layers by immersion in toluene at 50 °C for 12 days, however observing damage to the silicon wafers attributable to the pressure exerted by the swelling of EVA [39]. These studies highlight how the treatment times with traditional organic solvents are typically long, constituting one of the main limitations of this category of processes. To accelerate dissolution and reduce processing times, several authors have integrated solvent action with energy assistance techniques. Kim and Lee achieved complete dissolution of EVA in o-dichlorobenzene at 70 °C with 900 W ultrasonic irradiation for only 30 min, without causing damage to the solar cells, demonstrating how ultrasonic irradiation allows for a drastic reduction in time compared to passive immersion [18]. Królikowski et al. combined moderate heating at 170 °C to separate the glass by softening the EVA with subsequent chemical delamination in toluene at 35 °C for 35 min using ultrasonic bath and mechanical agitation, obtaining separate fractions of EVA, PVDF, and PET through washing and sieving processes [45]. Wang et al. performed a chemical delamination by immersing in p-toluene sulfonic acid (PTSA) at 80 °C for 2 h using 800 W ultrasound, without damaging glass, silicon, and backsheet [58].

Green and low-toxicity solvents - In response to environmental and safety concerns associated with chlorinated solvents, a growing number of studies have explored alternative agents with more favourable toxicological profiles [60]. D-limonene, a natural terpene extracted from citrus fruits, has proven effective in swelling and detaching EVA layers in 30 min at 70 °C when combined with 800 W ultrasonic irradiation, showing complete efficacy up to three reuse cycles [61]. N-methyl-2--pyrrolidone (NMP) achieved complete delamination at 150 °C in 60 min without releasing toxic gases or damaging the glass or silicon wafer [62]. A similar approach was proposed by Lu et al., who employed N, N-dimethylacetamide (DMAC) in a three-stage sequential process in the same solvent: immersion at 25 °C for 5 min for the removal of the fluorinated coating of the backsheet; heating at 160 °C for 10 min for the swelling of EVA and the separation of glass; ultrasonic irradiation at 20 kHz and 800 W for 10 min for the complete separation of backsheet, EVA, and bonding wires from the solar cell [63]. Li et al. used the green reagent DMPU ($C_6H_{12}N_2O$) at 160 °C with an ultrasonic field at 900 W for 20 min, achieving complete layer separation with less EVA swelling compared to traditional reagents and with the possibility of recovering the solvent after use [64]. A particularly interesting direction for the long-term sustainability of chemical processes is represented by regenerable organic solvents. Lu et al. demonstrated that isopropyl myristate (IPM), used at 140 °C with 800 W ultrasonic irradiation, allows for the selective separation of the front glass while preserving the underlying cells, with the possibility of reusing the solvent for over a hundred consecutive cycles without significant alteration of its properties [65]. In the same study, diethyl malonate (DEM) was used at 60 °C for the removal of the EVA backsheet, maintaining operational stability for about ninety cycles before requiring regeneration [65]. These green solvents represent a promising research direction, although their higher average cost compared to traditional solvents remains a limiting factor for industrial-scale implementation.

Deep Eutectic Solvents (DES) - Deep eutectic solvents represent a new class of low-melting-point mixtures composed of hydrogen bond donors and acceptors, characterised by low toxicity and high biodegradability. Yu et al. demonstrated the applicability of a DES based on choline chloride and oxalic acid (ChCl-OAD) for chemical delamination and simultaneous leaching of aluminium from the solar cell by immersion at 175 °C for 7.5 h, highlighting that DESs have low costs and can be

recycled, although with long process times that limit their industrial applicability [66]. Yang et al. proposed a hydrophobic DES system based on menthol and decanoic acid ([Men][DecA]), operating at 80 °C for 2 h, which allows for complete delamination and can be regenerated and reused through a simple phase change procedure: after chemical delamination, EVA is separated from the solvent and the DES is transformed into a hydrophilic phase by adding a 25 % wt aqueous ammonia solution, and then regenerated by adding HCl to the liquid phase [67]. This approach to solvent regenerability represents a significant advantage over traditional non-recoverable organic solvents.

4.5. Advanced delamination processes

The processes discussed in this section are defined as "advanced" not in reference to their degree of technological maturity but rather to their intrinsic technological complexity. Each of these processes requires specialised equipment or unconventional operating conditions that distinguish them from the conventional mechanical, thermal, and chemical processes discussed in the previous sections and significantly affect their scalability and investment costs.

Laser irradiation - Laser irradiation is a precision, non-contact technique for the selective detachment of the EVA layer from the surface of the silicon cell. By directing a pulsed laser beam in the near-infrared onto the rear surface of the module, the laser energy induces a highly localised transient thermal effect at the EVA-silicon interface, disrupting the adhesion between the two layers through a combination of rapid heating and mechanical stress induced by differential thermal expansion, without causing damage to the silicon cell or the silver contact grids. Anwar et al. showed that nanosecond laser pulses at 355 nm allow the subsequent mechanical detachment of the glass–EVA layer from the silicon cell without damaging the silver metallisation grids [68]. Li et al. confirmed that laser irradiation at 1064 nm increases the temperature in the adhesion interface region of EVA, reducing adhesion and allowing the mechanical detachment of solar cells while ensuring their integrity, with a recovery of 45 % of the total EVA present in the module [1]. Although these approaches offer high precision and low thermal impact on the rest of the module, their productivity is currently limited by the sequential nature of the scanning, making scale-up to industrial volumes technically challenging.

Electrohydraulic fragmentation (EHF) – Electrohydraulic fragmentation is a process in which the module is immersed in water and subjected to high-voltage electric discharges that generate intense shock waves. These shock waves preferentially propagate along the interfaces between materials of different mechanical impedances, inducing selective fractures at the boundaries between glass, EVA, and silicon through the combination of impulsive pressure effects, hydrodynamic cavitation, and shear stresses at the interfaces. Compared to conventional mechanical crushing, EHF produces a more selective release of components and achieves a higher enrichment of metals in the fine fractions [69,70]. Padhamnath et al. proposed a process where the modules are first subjected to mechanical milling with a rotary crusher and subsequent sieving into three granulometric fractions (>5 mm predominantly containing EVA, cells, and glass; 1–5 mm containing glass fragments; and <1 mm containing glass, silicon, and metals). Subsequently, the coarser fraction (>5 mm) is treated with EHF using shock waves in water at a voltage of 50 kV for 4 min, achieving selective delamination of the module layers through preferential fracture at the interfaces between materials with different mechanical impedances [69]. The same research group applied EHF in water for 240 s on panels previously cut into 2.5 × 2.5 cm pieces, obtaining a coarse powder (>250 μm) and a fine powder (<250 μm) from the subsequent size separation, with the second one enriched in metals and silicon and sent to the subsequent leaching and recovery phases [70]. Both studies emphasise the low environmental impact of the process, which does not require chemical reagents in the delamination phase and allows for the treatment of even damaged or deformed modules, overcoming one of the main limitations of other methods such as the hot knife.

Supercritical CO_2 - The use of supercritical CO_2 as a delamination agent exploits the ability of CO_2 under supercritical conditions to diffuse into the polymer matrix of EVA, modifying its mechanical properties. In particular, Briand et al. demonstrated that the absorption of supercritical CO_2 in EVA at a pressure of 150 bar and a temperature of 75 °C induces a controlled swelling of the polymer, while the subsequent rapid depressurisation at a rate of 2.7 bar/s generates the nucleation and growth of bubbles within the polymer matrix, creating internal mechanical stresses sufficient to separate the layers of the module [71]. The process does not require the use of toxic chemical solvents and does not generate hazardous by-products, representing a clean approach for the delamination of PV modules. The necessity to operate at high pressure in dedicated pressurised reactors, however, represents the main technical and economic barrier to its industrial-scale implementation.

Subcritical water and solvothermal treatments - This category encompasses delamination processes conducted in a pressurised closed reactor at temperatures above the solvent's boiling point, where the thermal and chemical effects act simultaneously on the polymeric matrix of the module. The high temperature and pressure modify the properties of the solvent, increasing its diffusivity and penetration capacity into the EVA matrix, inducing a controlled swelling that reduces adhesion between the layers and allows for separation. Birtürk and Celiktas have demonstrated that treatment with pure subcritical water at 200 °C and 100 bar for 30 min allows the solvent to penetrate the EVA matrix, causing controlled swelling and structurally degrading the backsheet, enabling the subsequent manual separation of the EVA layer without generating toxic byproducts [72]. The process is distinguished by its intrinsically clean nature as the solvent is pure water, it does not require additional chemical reagents, and it does not produce hazardous gas emissions [72]. Yan et al. proposed the use of a KOH-ethanol solution in a pressurised reactor at 200 °C for 3 h, exploiting the superior wetting properties of ethanol compared to water to facilitate the penetration of OH^- ions at the cell-EVA-glass interface and reducing the swelling times of the matrix, achieving a recovery of 96.27 % of the silicon wafers [36]. Zhang et al. adopted a two-stage approach in a pressurised reactor with an initial immersion in citric acid or malic acid at 180 °C for 30 min to separate the rear EVA layer, followed by a second immersion in Na_3PO_4 at 200 °C for 60 min to remove the front EVA and silver grids, achieving complete delamination with low-toxicity reagents [73]. Finally, He et al. proposed a sequential process characterised by immersion in anhydrous ethanol at 200 °C for 15 min in a solvothermal environment for the removal of the rear EVA and the aluminium electrode, followed by immersion in Na_2CO_3 at 200 °C for 120 min for the removal of the front EVA layer and the silver grids, achieving complete delamination with minimal damage to the recovered materials [19]. All these approaches share the advantage of operating without halogenated or highly toxic solvents, with reagents that are often recoverable and reusable, positioning themselves as one of the most promising research directions for the development of chemically sustainable delamination processes on an industrial scale.

Table 2 summarises the analysed delamination processes.

4.6. Comparative discussion

The individual delamination and separation techniques are compared in Table 3. No single route is superior on all counts, and each involves a distinct balance between the quality of the recovered materials, the processing time and the environmental burden. Solvent-based chemical dissolution and selective advanced techniques such as laser debonding act gently on the laminate and recover the silicon cells undamaged, but they are slow or depend on specialised equipment. Thermal pyrolysis removes the encapsulant most completely and recovers glass and cells, at the expense of high energy consumption and, when the fluoropolymer backsheet is co-treated, of fluorinated emissions. Purely mechanical crushing is the fastest and simplest option, but

Table 2
Analysed studies on the delamination processes of c-Si PV modules, indicating the category of treatment adopted (Mechanical – M; Thermal – T; Chemical – C; Advanced – A), the specific method, the main operating conditions and the characteristics of the processes.

Ref.	Process	Specific Technique	Method	Features
[27]	M	Shredding + electrostatic separation	Shredding <2 mm; electrostatic separation, field at 24 kV, rotation at 30 rpm	Separation into conductive and non-conductive fractions
[20]	M	Milling + electrostatic separation	Milling with blade mill (4 mm and 2 mm screens); electrostatic separation with high-voltage rotating roller (24–28 kV, 30–80 rpm) into three fractions (conductors, semiconductors, non-conductors)	>90 % of metals concentrated in the conductive fraction
[47]	M	Milling + size-based separation	Blade mill at 400 W, 15 min → particles <6.35 mm; sieving into 3 fractions: >4 mm (33.71 % polymers); 0.5–2 mm (99.37 % Cu, 76.85 % glass); <0.25 mm (94.12 % of total Ag)	Incomplete polymer separation; contaminated glass
[42]	T	Thermal oxidation	Heating at 500 °C, 90 min, oxidising atmosphere (EVA and polymer degradation)	Complete polymer degradation; 20× metal concentration for subsequent processing
[43]	T	Two-step pyrolysis	Heating at 150 °C, 5 min (manual backsheet removal); pyrolysis at 500 °C, 1 h (EVA decomposition)	Intact backsheet recovered; 99 % EVA degradation in pyrolysis
[28]	T	Two-step thermal treatment	Heating at 170 °C, 10 min, muffle furnace (manual backsheet removal); thermal treatment at 600 °C, 18 min	Complete EVA removal. Alternative: single heating at 600 °C, 33 min total
[41]	T	Pyrolysis	Pyrolysis 600 °C, 7 min, heating rate 10 °C/min	Complete layer separation; polymer decomposition >98 %
[46]	T-C	Cryogenic + pyrolysis + KOH	Cooling −40 °C, 3 min; heating 650 °C, 30 min; KOH, 80 °C	Reduced adhesive strength and EVA decomposed via thermal treatment; EVA reusable after ethanol washing
[2]	M-T	Mechanical backsheet removal + thermal	Mechanical backsheet removal with micro-grinder (cutter Ø 6.5 mm, router stand h 3.9 cm); heating at 500 °C, 20 min (initial T 50 °C, heating rate 9 °C/min)	Mechanical treatment reduces subsequent thermal treatment time; polymer removal 99.6 %
[23]	M-T	Milling + pyrolysis + sieving	Milling with knives mill; pyrolysis at 500 °C, heating rate 10 °C/min; sieving	Polymer fractions completely degraded; sieving into fractions <0.5 mm/ 0.5–1 mm/ >1 mm
[5]	M-T	Thermal + size-based (slotted sieving)	Heating at 500 °C, 60 min (EVA and polymer removal); slotted sieving (Si/ glass separation by particle shape)	Modules cut into 10 × 10 mm for sieving; recovery of 90 % of module weight (excl. frame, polymers, other components)
[40]	M-T	Milling + sieving + pyrolysis	Milling with blade mill; sieving into 3 fractions (<0.5 mm/ 0.5–1 mm/>1 mm); pyrolysis at 500 °C, 30 min, heating rate 15 °C/min	Polymer removal 99 %
[44]	M–T	CNC mechanical removal + thermal oxidation	Mechanical backsheet removal with CNC milling machine (18,000 rpm, feed rate 4000 mm/min, abrasion depth 0.8 mm, ~8 min/ panel); thermal treatment at 500 °C, 1 h, oxidising atmosphere (U = 0.5), gas flow rate 24 L/h	Elimination of HF and fluorinated compound emissions; significant VOC reduction compared with conventional thermal treatment; complete EVA degradation
[18]	C	o-Dichlorobenzene (ultrasonic)	O-dichlorobenzene 3 M, 70 °C, ultrasonic irradiation at 900 W, 30 min	Intact cells; no toxic gas emissions
[61]	C	Limonene (green solvent, ultrasonic)	Limonene 0.1 M, s/L 1/15, 70 °C, ultrasonic field 800 W, 30 min	Complete separation of glass and backsheet from EVA
[34]	C	Trichloroethylene (TCE)	Trichloroethylene (TCE), 80 °C, 10 days	Silicon cell recovered without damage
[35]	C	Trichloroethylene (TCE)	Trichloroethylene (TCE), 70 °C, s/L 1:7.44, 8 h	Effective separation of module layers from EVA
[57]	C	Toluene	Toluene, 50 °C, 3 days, mechanical stirring at 600 rpm	Toluene recovered and reused via chemical distillation
[58]	C	p-Toluenesulfonic acid (PTSA, ultrasonic)	p-Toluene sulfonic acid (PTSA) 3 %, 80 °C, 2 h, ultrasonic field 800 W	Complete delamination; intact glass, Si and backsheet
[62]	C	N-methyl-2-pyrrolidone (NMP)	N-methyl-2-pyrrolidone (NMP), 150 °C, 60 min	No NO_x or toxic gas emissions; green, low-cost solvent; undamaged glass and Si wafer
[66]	C	Deep eutectic solvent (ChCl-OAD)	DES ChCl-OAD, 175 °C, 7.5 h (delamination + Al leaching from cell)	Non-toxic green solvent; low-cost and recyclable DES

(*continued on next page*)

Table 2 (*continued*)

Ref.	Process	Specific Technique	Method	Features
[67]	C	Deep eutectic solvent (menthol/ decanoic acid)	DES [Men][DecA] (menthol/decanoic acid 1:1), 80 °C, 2 h	Reusable DES: separation of EVA from the solvent, conversion of DES to hydrophilic phase with 25 wt % aqueous amine solution, regeneration of DES with HCl
[64]	T-C	DMPU solvent, ultrasonic + heating	DMPU, 20 min, 160 °C, ultrasonic field 900 W, s/L 1/ 12 g/ml	DMPU prevents solar cell damage and can be recovered
[59]	M-T-C	Thermal + toluene + calcination	Mechanical removal of glass and backsheet with pincers after halogen lamp heating, 3 min; toluene/H_2O 1:1, 80 °C, 120 min; centrifugation at 3600 rpm, 30 min; calcination at 500 °C, 1 h	Chemical treatment removes 72 % of EVA; calcination eliminates residual EVA
[45]	M-T-C	Thermal softening + toluene (ultrasonic)	Heating at 170 °C (EVA softening + mechanical force) for glass separation; toluene at 35 °C, 35 min, ultrasonic bath + mechanical stirring at 500 rpm	Glass recovered as millimetre-sized fragments (physical damage); separated EVA, PVDF and PET fractions via washing and sieving
[63]	T–C	DMAC solvent + ultrasound	DMAC, 25 °C, 5 min (removal of fluorinated coating from backsheet); DMAC at 160 °C, 10 min (EVA swelling and glass separation); ultrasound at 20 kHz, 800 W, 10 min (separation of backsheet, EVA and bonding wires from the cell)	Chemical delamination in 3 stages with the same solvent; 99 % reduction in EVA adhesion
[71]	A	Supercritical CO2	Supercritical CO_2, absorption into the polymer at 150 bar and 75 °C; rapid depressurisation at 2.7 bar/s	CO_2 absorption → polymer swelling; rapid decompression → bubble nucleation + mechanical stress → separation of module layers
[69]	M-A	Milling + sieving + electrohydraulic fragmentation	Milling with rotary shaft crusher; sieving into 3 fractions (>5 mm: EVA + cells + glass; 1–5 mm: glass; <1 mm: glass + Si + metals); electrohydraulic fragmentation (EHF), shock waves in H_2O, 50 kV, 4 min (>5 mm fraction)	EHF induces fractures at interfaces between materials with different mechanical impedance; low environmental and economic impact
[68]	M-A	Laser debonding	Laser debonding (selective transient melting at the EVA–Si interface); 355 nm, 5 ns, 10 Hz, scanning at 30 mm/ s; manual separation of EVA + glass from cell	Separation of EVA + glass from the cell; intact Ag grids
[1]	M-T-A	Thermal + NIR laser debonding	Rear-side heating at 500 °C, few seconds; manual backsheet removal; NIR pulsed laser at 1064 nm; mechanical EVA removal	Localised thermal treatment; 45 % recovery of total EVA
[72]	C-A	Subcritical water	Subcritical water, 200 °C, 100 bar, 30 min (EVA swelling, backsheet degradation, glass separation); manual EVA removal	Subcritical water acts as a green solvent and penetrates the polymer matrix; clean process, no toxic gases
[36]	T-C-A	Solvothermal (KOH-ethanol) + thermal	KOH-ethanol, 200 °C, 3 h, s/L 55 g/L, [KOH] 0.2 mol/L; heating 550 °C	Si wafer recovery 96.27 %; thermal treatment for elimination of persistent organic residues
[19]	M-T-C-A	Thermal + solvothermal (ethanol/Na2CO3)	Heating at 170 °C, 5 min (mechanical separation of glass and backsheet); anhydrous ethanol under solvothermal conditions at 200 °C, 15 min (rear EVA + Al electrode); Na_2CO_3 0.3 mol/L under solvothermal conditions at 200 °C, 120 min (front EVA + Ag grids)	Low environmental impact; undamaged materials
[73]	C-A	Organic acids (solvothermal)	Citric or malic acid 0.6 mol/L, 180 °C, 30 min (rear EVA separation); Na_3PO_4 0.4 mol/L, 200 °C, 60 min (front EVA and Ag grids separation)	Complete delamination; low-toxicity reagents, reusable for up to 5 cycles in the first stage

it destroys the laminate and yields mixed fractions of low purity that require further refining.

These characteristics are reflected in very different levels of technological maturity. Mechanical and thermal treatments are the routes that have most widely reached commercial scale, either as stand-alone processes or as the delamination stage of integrated recycling plants [24,75], and the hot-knife method provides an industrially available route for the non-destructive recovery of glass [54]; by contrast, most chemical and advanced routes have so far been demonstrated only at laboratory or pilot scale. The mature routes achieve throughput either by sacrificing the quality of the recovered materials, as in mechanical crushing, or by incurring high energy use and secondary emissions, as in thermal treatment, whereas the routes that are simultaneously gentle, selective and low-polluting remain the least developed. Advancing these cleaner routes towards a scalable and industrially viable form, for instance within integrated schemes that couple a mild delamination step with efficient downstream separation, is a central requirement for the maturation of c-Si module recycling.

Table 3
Qualitative comparison of the delamination and separation techniques for c-Si PV modules.

Category	Specific technique	Driving mechanism	Target layer/ interface	Advantages	Limitations and by-products	Ref.
Mechanical	Crushing and milling	Compressive, shear and impact comminution	Whole laminate	Simple, scalable, reagent-free	Incomplete polymer removal; mixed low-purity fractions; losses	[23, 40,47, 69]
Mechanical	Size-based separation	Particle-size classification	Crushed mixture	Low cost; concentrates Ag and Si in the fine fractions	Pre-concentration only, no purification	[5,40, 47,69]
Mechanical	Magnetic/eddy-current separation	Magnetic susceptibility and induced currents	Crushed metallic fractions	Reagent-free and dry; removes the ferrous fraction and recovers non-ferrous metals (Al, Cu)	Coarse separation; most effective on coarser particles; acts only on the metallic fractions and does not separate individual non-ferrous metals	[74]
Mechanical	Electrostatic separation	Differential conductivity and surface charge	Crushed mixture	Dry; separates conductors from glass and polymer	Recovered Si of low purity; sensitive to size and humidity	[20, 27]
Mechanical	Hot knife	Local thermal softening of EVA	Glass-EVA interface	Intact glass; fast; no combustion CO2	Cells may break; not for damaged modules; EVA residue	[26, 52]
Mechanical	Water-jet cutting	High-pressure (abrasive) water jet	Glass-EVA interface	Clean intact glass; reagent-free; no CO2	High water use; cells fragmented; wastewater	[75]
Thermal	Pyrolysis	Thermochemical decomposition of polymers (inert)	EVA encapsulant	High polymer removal; intact glass and cells	Fluorinated and volatile by-products; energy-intensive	[23, 40,41, 43]
Thermal	Thermal oxidation/ combustion	Oxidative degradation of polymers	EVA encapsulant	Complete polymer removal	Risk of cell and metal oxidation; energy-intensive	[42, 44]
Thermal	Thermal softening	Moderate heating to reduce EVA adhesion	Glass-EVA interface	Mild; enables mechanical glass separation	Residual EVA; requires a mechanical step	[28, 45]
Chemical	Organic solvents (TCE, toluene, NMP, o-DCB)	EVA dissolution and swelling	EVA encapsulant	Recovery of intact cells	Long times; solvent toxicity; liquid effluents	[18, 34,35, 57,62]
Chemical	Green solvents (limonene)	EVA dissolution	EVA encapsulant	Lower toxicity	Long times; cost	[61]
Chemical	Deep eutectic solvents	EVA swelling and depolymerisation	EVA encapsulant	Low toxicity; biodegradable; reusable	Long times; high viscosity	[66, 67]
Chemical	Acids (PTSA, citric/ malic)	Weakening of EVA adhesion	EVA encapsulant	Mild; recyclable reagents	Pre-treatment; effluents	[58, 73]
Advanced	Supercritical CO2	Diffusion into EVA and rapid depressurisation	EVA encapsulant	Reagent-free; fast	High-pressure equipment	[71]
Advanced	Subcritical water/ solvothermal	Pressurised hot water or solvent degradation	EVA encapsulant	Low-toxicity medium; effective	High pressure; possible glass corrosion	[19, 36,72]
Advanced	Electrohydraulic fragmentation	Shockwaves in liquid at material interfaces	Laminate interfaces	Selective liberation; high-purity Si; low pollution	Specialised equipment; dust	[69]
Advanced	Laser debonding	Selective melting at the EVA-Si interface	EVA-Si interface	Selective; intact cells	Specialised; low throughput	[1,68]

5. Recovery of materials from EoL c-Si PV modules

5.1. From delamination to material recovery

After disassembly and delamination, the laminated core of the module is in a state where valuable components, such as silicon cells, silver and aluminium metal contacts, and copper ribbons, have been released from the polymeric matrix and are accessible for subsequent recovery operations. In addition to these cell components, the tempered glass, which is separated during the delamination step and represents the largest fraction of the module by mass, constitutes a further material to be recovered and is treated in a dedicated subsection. Recovery of materials is essential for the sustainability of the PV sector both from an environmental perspective, preventing waste from polluting the environment through landfill accumulation, and from an economic perspective, enhancing recycled materials by reintroducing them into production chains as secondary raw materials [6,38,76].

The recovery of materials from c-Si modules is primarily based on hydrometallurgical processes, which use acidic or basic solutions to selectively leach the metals present on the surface of solar cells, followed by separation and purification operations of the leachate solution, such as chemical precipitation, electrodeposition, liquid-liquid extraction, to obtain the metals in pure form [6,38,77]. The hydrometallurgical approach is widely applied and studied in the literature for its high selectivity, low energy consumption, and high control over the purity of the recovered products, although it generates liquid waste that requires dedicated treatment before disposal [6,17]. The typical recovery sequence involves the progressive removal of metal layers from the cell surface through successive leaching with increasingly aggressive reagents, starting with the more easily soluble metals such as aluminium and silver, and culminating in the purification of the silicon wafer [7,38, 76].

A critical aspect of this phase is the choice of leaching reagents. Nitric acid (HNO_3) is the most widely used lixiviant for the simultaneous dissolution of silver and aluminium, thanks to its high efficiency and the speed of the process [6,11,22,38,76,77]. However, HNO_3 generates toxic NO_x fumes during the reaction, requires dedicated abatement systems, and needs continuous replenishment to maintain its leaching effectiveness [78]. For these reasons, an increasing number of studies have explored less toxic and more selective alternative reagents, including ammoniacal solutions [78,79], peroxidic systems [78,80], deep eutectic solvents [65,81], and organic acids [80], as discussed in the following paragraphs.

The main leaching reagents used for metal recovery from c-Si cells and their reported findings are summarised in Table 4.

5.2. Silicon recovery

Silicon is probably the material of highest strategic value in c-Si modules. Its production from virgin raw materials is energy-intensive, its cost and limited market availability make it the most economically relevant component of the recycling process [34]. Moreover, its purity, which must reach solar grade (6N; 99.9999 %) for the manufacture of new cells, is difficult to restore once the cell has completed its life cycle [8,17,74,84,90,91]. The recovery of silicon from EoL modules requires the sequential removal of all layers covering the wafer: the rear

Table 4
Leaching reagents used for the recovery of metals from c-Si solar cells and their reported findings.

Reagent/system	Method	Targeted metal/layer	Typical conditions	Leaching efficiency	Recovery/purification method	Results (purity)	Ref.
Nitric acid (HNO_3)	Acid	Ag; Ag + Al	1–5 M, 20–140 °C	Ag >95 %, up to 100 % (140 °C, 2 h)	AgCl precipitation (HCl/NaCl) + reduction (hydrazine or ascorbic acid); electrolysis	Ag ~98.85 %; >99 % as Ag nanoparticles	[11,38,76,82,83]
Sulfuric acid (H_2SO_4)	Acid	Ag; Al	2–6 M, 25–60 °C	Al up to 99.77 %	$Al(OH)_3$ precipitation (NaOH)	Enables HF-free Si recovery (4N) as part of an acid + alkaline process	[77,84]
Hydrochloric acid (HCl, ± H_2O_2)	Acid	Cu (from solder ribbons)	~4 M, 60–80 °C	Selective Cu dissolution	Liquid–liquid extraction (TBP) + electrowinning	CuO	[85,86]
Sodium hydroxide (NaOH)	Alkaline	Rear Al electrode	1–5 M, 40–80 °C	Complete Al removal (6 min, 60 °C)	—	—	[84,87]
Potassium hydroxide (KOH)	Alkaline	Rear Al electrode	2 M – 40 wt%, 80 °C	Selective Al removal	—	—	[8,86]
Ammonia + H_2O_2 ($NH_3{\cdot}H_2O/H_2O_2$)	Other	Ag (selective)	room T–40 °C, 1–2 h, ± UV	Ag 99–99.9 %	Precipitation → Ag powder	Ag 99.99 %	[78,79]
Deep eutectic solvents + H_2O_2 (ChCl–oxalic; $FeCl_3{\cdot}6H_2O$–urea)	DES	Ag (and Al)	80 °C, 1–2 h	Ag 89–93.5 %; Al 100 %	Precipitation with water; DES recyclable	—	[65,81]
Glycine + H_2O_2	Other	Cu, Zn, Cd	25 °C	Selective co-recovery	Selective leaching/ precipitation	Purities >99 % each	[88]
$AlCl_3{\cdot}6H_2O$ + H_2O_2	Other	Ag and Al	80 °C, 30 min	Ag 95.32 %; Al 99.77 %	Simultaneous	—	[33]
Citric acid ($C_6H_8O_7$) + H_2O_2	Acid	Ag	70 °C, 2.5 h	—	AgCl precipitation + ascorbic-acid reduction	Ag 99.85 %	[80]
Bioleaching (cyanide, CN^-)	Bioleaching	Ag	microbial culture, 8 days	~44.7 %	—	—	[89]

aluminium electrode, the front silver metallisation grids, the ARC, and the p-n junction [4,8,74,84,90,91].

The removal of the rear aluminium electrode is typically carried out by leaching with basic solutions, such as sodium hydroxide (NaOH), exploiting the solubility of aluminium in an alkaline environment [4,8,87,91]. Subsequently, the silver grids are removed through acid leaching, as discussed in section 5.3. The removal of the ARC layer represents one of the most critical technical challenges of the process, and the most used reagents are HF [4,7], high-concentration and high-temperature phosphoric acid (H_3PO_4) [6,74,86,91], and NaOH [84]. Chen et al. demonstrated that etching with H_3PO_4 at 100 °C for 60 min allows for the complete removal of the ARC layer, resulting in solar-grade silicon, avoiding the use of HF [91]. Park and Park obtained silicon wafers with resistivity and carrier lifetime values equivalent to commercial wafers through sequential etching with H_3PO_4 at 160 °C for 60 min for the removal of the ARC and the p-n junction, confirming the feasibility of recovering reusable silicon to produce new cells [74]. The removal of the p-n junction is typically carried out with acidic mixtures containing HNO_3 and HF [4,7,90] or with NaOH [84,91], operating at temperatures and concentrations that allow for the controlled removal of a few micrometres of doped silicon without compromising the integrity of the wafer.

Klugmann-Radziemska and Ostrowski have demonstrated that sequential treatment with KOH at 80 °C for aluminium removal, followed by a mixture of HNO_3, HF, and CH_3COOH for ARC and p-n junction removal, allows the recovery of reusable silicon wafers for the production of new cells with conversion efficiencies ranging from 13 % to 16 % [8]. Wang et al. proposed a process using only two reagents, H_2SO_4 at 60 °C for silver removal and NaOH for aluminium and ARC removal, achieving silicon with 4N purity (99.99 %) without resorting to HF, representing a significant step forward towards safer and more sustainable processes [84]. Sah et al. used a sequential approach with differentiated reagents, employing KOH at 80 °C for aluminium removal, HNO_3 at 70 °C for silver recovery, HCl at 80 °C for copper separation, and finally H_3PO_4 at 170 °C for ARC layer removal [86]. An innovative approach was proposed by Lin et al., who used high-speed friction separation with quartz sand at 0.1 MPa to mechanically remove the back aluminium electrode, silver residues, and the ARC layer from the wafer surface, obtaining silicon without resorting to any chemical reagents in the surface layer removal phase [89].

5.3. Silver recovery

Despite accounting for less than 0.1 % of the module's total mass, silver represents up to 35 % of the overall economic value recoverable from the entire recycling process, so its recovery has received significant attention in the scientific literature [11,38,76]. The growing concern about the future availability of silver makes its recovery from EoL modules a priority both economically and strategically [6,79].

Silver leaching is carried out in the vast majority of studies using HNO_3 in various concentrations, from 1 M to 5 M, at temperatures ranging from 20 to 80 °C, with extraction yields typically exceeding 95 % [6,11,22,38,70,76,77,86,92]. Luo et al. achieved a silver leaching yield of 98.12 % with HNO_3 at 45 °C for 100 min [38]. Savvilotidou and Gidarakos achieved 89 % extraction with 30 % HNO_3 at 20 °C with constant stirring at 150 rpm for 1 h [22]. Kastanaki et al. demonstrated that hydrothermal leaching conditions with HNO_3 at 140 °C for 2 h allow for the achievement of 100 % silver extraction from both monocrystalline and polycrystalline modules [82].

In response to concerns related to the toxicity of HNO_3 and the generation of NO_x fumes, several studies have explored alternative reagents [33,65,78–81]. Zubas et al. proposed leaching with NH_3 + H_2O_2 at room temperature for 60 min, achieving silver extraction yields of 99-99.9 % without the generation of toxic fumes [78]. Chen et al. developed a selective leaching process with $NH_3{\cdot}H_2O$ and H_2O_2 at 40 °C for 2 h with UV irradiation at 365 nm, allowing for the selective extraction of silver while leaving other metals intact and obtaining silver powder with 99.99 % purity through subsequent precipitation [79]. Yang et al. employed a DES system (choline chloride–oxalic acid) with H_2O_2 at 80 °C for 2 h, achieving an 89.19 % leaching of silver with simultaneous dissolution of 100 % of aluminium: in this case, the DES acts both as a selective leaching agent and as a complexing agent for the dissolved metals [81]. Lu et al. have also proposed an interesting application of DES, and through a mixture of $FeCl_3{\cdot}6H_2O$ and urea at

80 °C they achieved a silver leaching efficiency of 93.5 % [65]. A distinctive approach is that proposed by Takaya et al., where silver contacts are pre-exposed through treatment with electric pulses before leaching with HNO_3 at 25 °C, achieving a recovery yield of 95 % and the simultaneous recovery of copper busbars [55]. Finally, Su et al. employed an etching system based on $AlCl_3{\cdot}6H_2O$ with H_2O_2 at 80 °C for 30 min, achieving the simultaneous removal of silver and aluminium from the cells with yields of 95.32 % and 99.77 %, respectively, without resorting to strong acid reagents [33].

The recovery of silver from the leaching solution primarily occurs through precipitation as AgCl by adding HCl or NaCl, followed by reduction to metallic silver using reducing agents such as hydrazine hydrate or ascorbic acid [6,11,38,76,93]. Días et al. obtained a silver concentration of 94 % through mechanical milling, sieving the fine fraction (<0.5 mm), and subsequent leaching with 64 % HNO_3 and precipitation with 99 % NaCl [11]. Chen et al. achieved a purity of the recovered silver of 98.85 % with an efficiency of 99.7 % through leaching with HNO_3 followed by precipitation with HCl and reduction with hydrazine [76]. A more sustainable alternative to hydrazine hydrate as a reducing agent was proposed by Zheng et al., who used ascorbic acid at 40 °C for 30 min to reduce the precipitated AgCl to metallic silver with an efficiency of 99.57 %, obtaining silver powder with a purity of 99.85 % [80]. Other methods have been explored as alternatives to precipitation, such as the cementation of silver by exchange with copper as a less noble metal, achieving direct precipitation without the need for chemical reduction stages [92]. A particularly innovative approach is that proposed by Choi et al., who used nanosecond pulsed laser irradiation at 355 nm on a suspension of Ag_2O obtained by leaching with HNO_3, producing spherical silver nanoparticles with a purity greater than 99 % and opening up high value-added recovery prospects for the metal [83].

A radically alternative research direction is represented by the bioleaching proposed by Lin et al., who employed cyanide ions produced by microorganisms cultured for 8 days as a biological leaching agent for silver; although the yield is lower than conventional chemical approaches, the complete absence of acidic reagents and the biocompatibility of the process make it a particularly interesting option in the perspective of zero-emission toxic effluent processes [89].

Beyond these hydrometallurgical routes, silver can also be recovered by thermal, or melting, approaches, in which the crushed cell material is heated to a high temperature to liberate the silver. In one reported route it is first heated to about 700 °C to remove the aluminium and then to around 960 to 1000 °C, near the melting point of silver, to separate the silver and the polysilicon [94]. Such high-temperature routes avoid the acids and effluents of the hydrometallurgical processes but are highly energy-intensive, whereas hydrometallurgical routes are more selective and reach high silver purity at lower temperature, at the cost of chemical reagents and waste-acid management.

5.4. Aluminium recovery

Aluminium is used in c-Si modules for both the rear electrode of solar cells, which is a thin layer deposited on the entire rear surface of the wafer, and the module's structural frame. The aluminium frame is recovered separately during the disassembly phase described in Section 4, while the rear electrode requires chemical etching operations on the cell surface [4,6,8,38,77,81].

The leaching of aluminium from the back electrode is predominantly carried out with basic NaOH or KOH solutions, exploiting the solubility of aluminium in an alkaline environment to selectively dissolve it without significantly attacking the underlying silicon [4,8,70,86,87,91]. Theocharis et al. achieved 99.77 % aluminium extraction with H_2SO_4 at 25 °C [77]. Kastanaki et al. achieved aluminium leaching yields between 85 % (monocrystalline silicon) and 88 % (polycrystalline silicon) through hydrothermal leaching with HNO_3 at 140 °C for 2 h [82]. Jung et al. recovered 94 % of the aluminium by precipitation as $Al(OH)_3$ in a basic environment followed by calcination at 1200 °C to obtain high-purity Al_2O_3 [6]. Chen et al. achieved an aluminium recovery efficiency of 98.9 % through leaching with HNO_3 followed by leaching with KOH to remove residual impurities [76].

Finally, Alsulami et al. proposed the leaching of aluminium with NaOH at 60 °C for 6 min as the first stage of an environmentally friendly process that does not require HF or HNO_3, achieving the complete dissolution of the back electrode with minimal effluent generation [87].

5.5. Copper, tin and lead recovery

Copper, tin, and lead are found primarily in c-Si modules' solder ribbons, which are strips of copper coated with Sn-Pb alloys that connect the cells in series within the module. Although they represent a minor fraction of the total mass of the module (about 1–1.3 %), their recovery is relevant both for the economic value of copper and for the need to remove lead, a toxic metal whose release into the environment must be prevented [6,76]. Tin, in particular, is classified as a critical raw material and is the primary constituent of that interconnection solder [95]. As photovoltaic deployment expands, the demand for tin is expected to rise appreciably, and the recycling of EoL modules has been identified as one of the most effective levers to limit the projected supply shortfall [95].

Chen et al. separated copper from the ribbons by leaching in HCl with H_2O_2 at 60 °C for 1 h to dissolve the Sn-Pb coating, followed by liquid-liquid extraction with TBP (tributyl phosphate) to separate the copper from the solution and subsequent electrowinning, obtaining CuO with an efficiency of 99.4 % [76]. Tin and lead are precipitated as hydroxides and calcined at 400 °C and 550 °C, respectively, to obtain SnO_2 and PbO with purity greater than 99 % [76]. Jung et al. recovered 79 % of copper through liquid-liquid extraction followed by electrowinning in H_2SO_4 [6]. Kavousi and Alamdari adopted a glycine leaching approach at 25 °C with H_2O_2 for the selective recovery of copper, zinc, and cadmium, achieving purities greater than 99 % for each metal [88].

5.6. Glass recovery

Glass constitutes the largest fraction of a c-Si module, representing between 70 % and 76 % of its mass [5,20,32], yet it contributes only marginally to the economic value of recycling, which is concentrated in the much smaller metallic fraction [75]. This creates a characteristic tension, in that the low market value of the glass discourages investment in its high-quality recovery, while, being the main component by mass, glass is decisive both for diverting the largest fraction of the waste stream from landfill and for meeting the ambitious EU recovery target of 80 %, which a strategy focused only on the metals cannot reach [96]. Depending on the availability of a secondary market, glass can therefore turn from a source of revenue into a significant economic liability for the recycler [97].

The recovery of glass is also supported by the strain on the primary supply of solar glass. Terawatt-scale PV deployment would demand of the order of 89 Mt of glass per year, some 3.7 times the current output, a supply that depends on low-iron sand whose deposits are still poorly mapped and on energy-intensive, largely fossil-fuelled manufacture, so that recovering and reusing EoL glass relieves pressure on a constrained and emission-intensive virgin chain [98].

Two contrasting approaches to glass recovery coexist. In destructive routes, the module is crushed and the glass is recovered as cullet mixed with residual encapsulant and with fine fractions of silicon and metals [40]; sieving concentrates the glass into specific size classes [40], but the resulting cullet is of limited purity. In non-destructive routes, based on the hot-knife method [26,52], water-jet cutting [75] or a careful thermal or chemical decomposition of the encapsulant, the tempered glass sheet is separated intact together with undamaged wafers and aluminium frames [12], preserving its value and avoiding the energy penalty of breaking and reprocessing it [75]. Thermal decomposition, and pyrolysis in particular, is often favoured for its simplicity and because, carried

out in an oxygen-deprived environment, it decomposes the organic components while leaving the intact glass and metals largely unaffected, unlike mechanical crushing, and avoids the hazardous and costly reagents of some chemical routes [8]. Reported glass recovery yields are high, of the order of 87 to 88 %, with solar-grade quality achieved in some cases [15,17]. The highest glass quality, however, is obtained by solvent treatment, which yields glass suitable as feedstock for new PV panels, whereas thermally treated glass can retain a surface residue of metals that limits its direct reuse [15,96]. The recovery of intact, high-purity glass, rather than of low-grade cullet, remains the more promising direction, provided that contamination by encapsulant and metals is controlled [9,23].

The environmental balance of the two routes has been quantified by life cycle assessment [99]. Introducing recovered cullet into new PV glass can reduce the global warming impact of glass manufacturing by up to about 71 %, but the cullet recovery process itself adds a burden, largely from the solvent step. The reuse of whole, intact glass emerges as the most favourable option, since it avoids the impact of producing new glass and markedly lowers fossil, metal and water depletion. Its residual impact is dominated by transport, which accounts for more than 80 % of the total [99], consistent with the central role of transport identified in the life cycle assessment section.

Beyond its mass, the recovery of PV glass is also significant because of the antimony it contains.

Solar glass, and in particular the rolled glass that dominates the market, typically contains between 0.1 and 0.5 wt% of antimony, added to improve the optical transparency and ultraviolet stability of the glass by oxidising ferrous to ferric iron [100]. Antimony is a scarce and critical raw material. It has been estimated that a terawatt-scale PV deployment would require of the order of 0.42 Mt of antimony per year for glass production alone, more than five times the current global output, with known reserves able to sustain the PV glass industry for only about five years. Recycling broken glass as cullet lowers the demand for virgin antimony, but at realistic recovery efficiencies of 30 to 60 % it could cover only some 2 to 11 % of the annual demand, so that the reuse of whole glass sheets recovered intact through the hot-knife and water-jet routes becomes a valuable complementary strategy. Recovering PV glass also brings an environmental benefit, since antimony can leach from landfilled modules into soil and groundwater, although the evidence available so far is mostly from laboratory tests [100].

Table 5 summarises studies that focus on the selective recovery of materials from c-Si PV panels.

5.7. Purity of recovered materials across recycling routes

The purity of the recovered materials depends strongly on the type of treatment applied, and the different routes are best understood by the role they play in the recycling chain rather than as competing alternatives. Purely mechanical processes carry out the liberation and bulk separation of the module. Beyond the bulk glass, aluminium and copper they have always recovered, recent commercial lines also report silicon and further metals, but at very different purities, with copper and trace metals sorted above 99 %, silicon recovered only at low grade, around 70 %, and silver and aluminium often of ore grade and sent to refineries for further upgrading [101]. Earlier surveys of mechanical plants report high overall recovery ratios, of the order of 95 %, but frequently do not disclose the purity of the recovered fractions [102].

Thermal treatments, and pyrolysis in particular, do not refine the metals, but they free clean glass and intact cells for the subsequent steps. In the reviewed studies glass is recovered at high yield, of the order of 87 to 88 %, and of solar-grade quality in some cases [15,17], although thermally treated glass may retain a surface residue of metals that limits its direct reuse [15]. The surveys, moreover, more often quantify the recovery than the purity of this fraction [103]. The high purity of the individual materials is achieved mainly through the chemical and

Table 5
Analysed studies on the material recovery of c-Si PV modules, indicating the category of treatment adopted (Mechanical – M; Thermal – T; Chemical – C), the specific processes, the main operating conditions and the recovered materials.

Ref.	Process	Recovered materials	Operating conditions
[88]	M-T-C	Ag 98 %; Cu 99.9 %; Pb 99.8 %; Sn 99.7 %; Cd 99 %; Zn 99.5 %; Al; Glass	Shredding and thermal treatment at 700 °C (glass + EVA removal); leaching + precipitation: Ag with HNO_3 0.5 M, 15 min; Cu, Zn, Cd with glycine 0.5 M, 25 °C, S/L 10 g/L, H_2O_2 1 %; Pb, Sn with glycine 1.5 M, 25 °C, 5 g/L
[38]	T-C	Ag 98.12 % (purity 99.8 %); Al 99.57 %; Si 96.03 %	Pyrolysis at 500 °C (EVA removal); leaching with HNO_3 3 M, L/S 16:1, 45 °C, 100 min; Ag precipitation with HCl → AgCl, dissolution in NH_3, reduction with hydrazine hydrate; ultrasonic cleaning of cells (removal of Al, Ag residues); cell purification with HF 20 wt%, 30 °C, 60 min
[77]	M-T-C	Si 85 %; Ag 95 % (purity 99.9 %); Al; Glass	Shredding to 4 mm; thermal treatment at 550 °C, 15 min (EVA removal); sieving (glass removal); milling to 90 μm; leaching with H_2SO_4 6 M for Al, 25 °C, S/L 5 %; precipitation of $Al(OH)_3$ with NaOH 5 M; leaching with HNO_3 5 M, S/L 30 %, 25 °C; precipitation of AgCl with NaCl/HCl; etching of Si wafer with NaOH 2.5 M, 25 °C
[8]	T-C	Si solar grade	Focus on chemical treatments of the cell (no pre-treatment, glass and metals); Al coating removal with KOH 30 %, 80 °C, 2–3 min; AR coating + n-p junction removal with HF/CH_3COOH/HNO_3 1:2:5, 40 °C, few min
[3]	M-T-C	Si; Al; Cu; Glass	Shredding <5 mm; thermal delamination at 80–90 °C (cell extraction from EVA); etching with KOH 30 %, 80 °C (rear Al); etching with HNO_3 35–40 %, 80 °C (front metallisation); etching with unspecified 3-component mixture (AR coating + junctions)
[33]	M-T-C	Ag 95.32 %; Al 99.77 %	Immersion in ethanol, 60 min (manual/mechanical backsheet removal); pyrolysis at 500 °C, 60 min (EVA removal); sieving 5 min (0.25/0.5/1/2/4 mm); fluidised bed separation (bed height 6 cm, air velocity 58.82 $m^3/(L{\cdot}h)$); etching of cells <4 mm with $AlCl_3{\cdot}6H_2O$ 0.6 mol/L + H_2O_2 2 %, 20 mL, 80 °C, 30 min (Al + Ag removal)
[7]	M-T-C	Si 90 %; Ag; Pb; Glass	Heating at 90–120 °C (backsheet and glass removal); thermal treatment at 650 °C, 30 min (EVA removal); etching with HNO_3 70 % (5 mL) + HF 40 % (0.5 mL), room T; 1 h for Pb, Cu, Ag; 24 h for AR layer
[4]	T-C	Si wafer and Si powder (solar grade); Ag; Al	Thermal delamination (EVA removal; separation of glass, Cu, Tedlar, Al frame, plastics); etching with HNO_3 40 %, 40 °C (Ag removal) + recovery via electrolysis; etching with KOH 30 %, 80 °C (Al removal); etching with HNO_3 65 % (83.33 mL) + HF 40 % (50 mL)

(continued on next page)

Table 5 (*continued*)

Ref.	Process	Recovered materials	Operating conditions
			+ CH_3COOH 99.5 % (50 mL) + Br_2 (1 mL), 70–80 °C, 10–12 s (AR coating + n-p junction removal)
[86]	M-T-C	Cu; Ag powder; Si	Thermal treatment at 480 °C, 30 min (EVA removal + glass separation); ultrasonic cleaning of cells + manual powder removal; etching with KOH 2 M, 80 °C (Al); etching with HNO_3 2 M, 70 °C, 1 h (Ag); etching with HCl 4 M, 80 °C, 4 h (Cu); H_3PO_4, 170 °C, 1 h (ARC)
[82]	T-C	Glass; Ag 100 %; Al 85 % m-Si, 88 % p-Si	Manual backsheet removal; thermal treatment at 600 °C, 20 min (EVA removal + separation of glass and metallic ribbons); milling to 0.5–1 cm^2; Ag leaching with HNO_3 2 N, L/S 10, 140 °C, 2 h; same conditions for Al
[22]	M-T-C	Ag 89 %	Thermal treatment at 550 °C, 1 h (EVA decomposition); leaching with HNO_3 30 %, 20 °C, stirring at 150 rpm, 1 h (Ag dissolution); Ag precipitation with HCl
[90]	T-C	Si solar grade	Thermal treatment at 500 °C (layer separation); etching with KOH 40 wt% (removal of metallisation and electrical contacts); etching with HF 48 %/CH_3COOH/HNO_3 70 % 1:2:5 (AR + n-p junction removal)
[81]	T-C	Si wafer; Al ~100 %; Ag 89.19 %; glass; Cu wires	Pyrolysis at 480 °C, 30 min (layer separation); cell leaching with DES (ChCl-oxalic acid) 2 mol/L + H_2O_2 2 mol/L, 80 °C, 300 rpm, s/L 1/100 g/mg, 2 h (Ag + Al removal); leaching with NaOH 1 mol/L, 300 rpm, 40 min (AR Si_3N_4 removal)
[76]	M-T-C	Si 99.9 % (purity 99.84 %); Cu 99.4 %; Sn 99.9 %; Pb 88.9 %; Ag 99.7 % (purity 98.85 %); Al 98.9 %; Glass	Toluene, 90 °C, 1 h (EVA swelling + mechanical glass removal); pyrolysis at 500 °C, heating rate 10 °C/min (EVA removal + ribbon/cell separation); leaching with HNO_3 5 M, 80 °C, 1 h, L/S 25 mL/g (99.4 % Ag + 76 % Al); leaching with KOH 1 M, 80 °C, 1 h, L/S 50 mL/g (residual impurity removal); PV ribbons in HCl 3 M + H_2O_2 6 %, 60 °C, 1 h (metallic coating dissolution + Cu separation); liquid–liquid extraction with TBP (Sn) and LIX984N (Cu); precipitation of metal ions as hydroxides; calcination at 400 °C (Sn), 550 °C (Pb), 700 °C (Cu)
[32]	M-C	Si 48.9 % (purity 91 %; Ag; Al; Glass	Crushing with high-speed hammer mill → coarse fraction >2.5 mm (polymers + ribbons) + fine fraction <2.5 mm (glass, Si, metals); electrostatic separation with rotating roller, field 15 kV, 30 rpm (Si recovery from fine powders 0.3–0.45 mm); HF washing (recovery of Si adhered to EVA)
[11]	M-C	Ag 94 %	Milling; sieving (>0.5 mm/<0.5 mm; fine fraction ~81 % Ag); leaching of fine fraction with HNO_3 64 %, room T, 2 h, magnetic stirring; Ag precipitation with NaCl 99 %

Table 5 (*continued*)

Ref.	Process	Recovered materials	Operating conditions
[17]	M-T-C	Al 94 %; Cu 90 %; Glass 88 %; Si 95 %; Ag 94 %	Mechanical treatment (glass removal); shredding; thermal treatment at 750 °C with emission abatement (EVA + backsheet decomposition); sieving (fine powders containing precious metals); leaching with HNO_3; electrolysis (selective Cu + Ag recovery)
[15]	M-C	Glass 87 % (solar grade)	Shredding + sieving into 4 fractions: >1 mm (glass + EVA + cells), 0.4–1 mm, 0.08–0.4 mm (glass + metals), <0.08 mm (glass + metals); cyclohexane, s/L 0.2 g/mL, 60 °C, 1 h (EVA swelling + layer separation, >1 mm fraction); leaching with H_2SO_4 2 M, 60 °C, 3 h, magnetic stirring (removal of metallic impurities + glass recovery from fine fractions)
[6]	T-C	Si 80 %; Ag 90 % (purity 99.99 %); Cu 79 %; Al 94 %; Pb 93 %; Glass	Thermal treatment at 480 °C, heating rate 15 °C/min (material separation + EVA decomposition); leaching with HNO_3 5 M, room T, 1 h, 200 rpm (dissolution of Al, Cu, Ag, Pb); Si wafer purification: H_3PO_4 90 %, 160 °C, 1 h (ARC SiNx removal) + KOH 45 %, 80 °C, 10 min (rear Al removal); Al recovery: precipitation of $Al(OH)_3$ in basic medium + calcination at 1200 °C; Cu recovery: liquid–liquid extraction with LIX84-I 20 % + H_2SO_4 150 g/L + electrowinning at 50 °C, 24 h; Ag recovery: precipitation with HCl 5 M → conversion to Ag_2O with NaOH 5 M → reduction with hydrazine hydrate in ethanol/H_2O → melting at 1100 °C, 2 h → electrolytic refining in HNO_3 0.06 M + $AgNO_3$ 0.3 M; Pb removal: precipitation of Pb$(OH)_2$ with NaOH 5 M → calcination at 500 °C, 1 h → reaction with Na_2S 5 M → precipitation as PbS
[74]	T-C	Si wafer, resistivity 1.6 - 10.1 Ω cm, carrier lifetime 1.785 μs	Unspecified thermal delamination; etching with H_3PO_4 90 %, 160 °C, 60 min (removal of ARC, SiNx, rear Al electrode); etching with HNO_3 + HF, 60 s (removal of Ag electrode, emitter layer, p-n junction)
[83]	M-T-C	Ag 98 % (purity >99 %)	Immersion in acetone, room T (backsheet removal); thermal treatment at 600 °C, 2 h, heating rate 10 °C/min (EVA removal); milling with agate mortar + sieving 300 μm; leaching with HNO_3 1 M, 60 min, S/L 75 g/L, 300 rpm; impurity removal with NaOH; irradiation with ns pulsed laser, 100 mJ, λ 355 nm, 60 min on Ag_2O suspension (spherical Ag particles)
[65]	C	Ag 93.5 %; Glass; EVA	Immersion in IPM (Isopropyl Myristate), 140 °C, 15 min, ultrasound 800 W (EVA swelling + glass separation); immersion in DEM (Diethyl Malonate), 60 °C, 45 min, ultrasound 800 W (weakening of EVA bonds +

(*continued on next page*)

Table 5 (*continued*)

Ref.	Process	Recovered materials	Operating conditions
			manual removal); Ag leaching with DES $FeCl_3{\cdot}6H_2O$ + urea 1:3, 80 °C, 60 min, mechanical stirring 400 rpm
[79]	C	Ag powder ~100 % (purity 99.99 %)	Cell already decapsulated. Leaching with $NH_3{\cdot}H_2O$ 1 % + H_2O_2, 40 °C, 2 h, UV irradiation at 365 nm (selective Ag extraction; other metals intact); precipitation → Ag powder
[87]	C	Al; Ag 93 %.	Pre-decapsulated modules; Al leaching with NaOH 2 M, 60 °C, 6 min (rear Al dissolution); immersion in $FeCl_3$ 0.8 M, 70 °C, 20–25 min, mechanical stirring 200 rpm (delamination of front Ag busbars)
[84]	T-C	Si (purity 99.99 %; 4N); Cu; Ag; Glass; Al	Pyrolysis at 500 °C, 3 h (decapsulation); ultrasonic cleaning at 100 kHz in deionised H_2O, 15 min; etching with H_2SO_4 5 M, 60 °C, 5 h (Ag removal); etching with NaOH 5 M, 12 h (Al + ARC removal)
[80]	M-C	Ag (purity 99.85 %)	Pre-decapsulated modules; milling at 400 rpm + sieving; Ag leaching with $C_6H_8O_7$ 2.35 mol/L + H_2O_2 30 % (437.5 mL/L), 70 °C, 2.5 h, L/S 10:1; Ag precipitation with NaCl → AgCl; AgCl dissolution in NH_3 + reduction with ascorbic acid, 40 °C, 30 min
[78]	T-C	Al 99 %; Ag 99-99.9 %	Thermal treatment at 500 °C, 1 h (decapsulation); Al leaching with NaOH, 40 °C, 60 min, S/L 1:20; Ag leaching with NH_3 + H_2O_2, room T, 60 min, S/L 1:10; alternative: simultaneous leaching of Ag + Al with HNO_3 + H_2O_2, 50 °C, 60 min, S/L 1:10
[91]	C	Si 96.37 % (solar grade); Ag 99.87 % (purity 88.74 %); Al	Pre-decapsulated modules; ultrasonic cleaning in anhydrous ethanol + drying at 70 °C, 2 h; Al leaching with NaOH 2.5 M, 70 °C, 30 min, L/S 25 mL/g (detachment of Ag grids); etching with H_3PO_4 8.76 M, 100 °C, 60 min (ARC SiNx removal); etching with NaOH 2 M, 50 °C until complete removal of doped surface Si (front sheet resistance = rear sheet resistance)
[93]	T-C	Intact solar cells (efficiency >50 %); Ag 95 %; Al 91 %	Thermal treatment at 200 °C, 2 h (reduction of EVA viscosity + generation of EVA/backsheet micro-gaps); immersion in toluene, room T, 120 h + ultrasound at 80 °C, 1 h, 720 W (backsheet removal); thermal treatment at 380 °C then 450 °C, 10 min (EVA degradation); Ag + Al leaching with HNO_3, 120 min; Ag precipitation with HCl + reduction with hydrazine; Al precipitation with $NH_3{\cdot}H_2O$ + calcination
[89]	T-C	Si wafer (carrier lifetime exceeded 4.9 μs); Ag; Al; Glass	Pyrolysis at 500 °C, 30 min, heating rate 10 °C/min (decapsulation); bioleaching with CN^-, 8 days (18 h culture) (Ag dissolution, efficiency 44.7 %); high-velocity fluid frictional separation with quartz sand, 0.1 MPa, 5 s on front surface + 10 s on rear surface (removal of rear Al electrode + Ag residues + SiNx coating; Si wafer recovery)
[92]	M-C	Ag > 90 % (purity >90 %); Si > 99 % (purity 99.67 %); Al 99 %; Cu	Pre-decapsulated modules; milling 15 min to −300 mesh; Ag + Al leaching with HNO_3, 30 °C, 3 h; residue washed and dried at 80 °C (Si recovery); Ag cementation with Cu (3× stoichiometry), 40 °C, 130 min, 500 rpm; Cu extraction with 10 vol% phenolic oxime (ACORGA M5640) in kerosene, 30 °C, 500 rpm (organic phase); stripping with H_2SO_4 4 M, 30 °C (Cu recovery)
[70]	M-C	Glass; EVA; Backsheet; Al; Ag; Si	Electrohydraulic fragmentation (EHF) in H_2O, 240 s (delamination); separation of output (metallic ribbons, polymers, glass, cell powders) into coarse fraction (>250 μm) and fine fraction (<250 μm); Al leaching from fine fraction with NaOH 1 M, 60 °C, 10 min; Ag leaching with HNO_3 49 %, 70 °C, 10 min; etching with HF 5 %, room T, 1 h (removal of glass powder + ARC from Si particles); immersion of polymer fraction in toluene, 90 °C, 24 h → NaOH + ethylene glycol, 150 °C, 2 h (separation of EVA from PET)
[55]	M-C	Cu busbars; Ag 95 %	Hot knife (glass removal); electric pulse treatment, 5 pulses in H_2O (exposure of Ag wires from encapsulated cells + recovery of Cu busbars and fine particles <1.18 mm with Ag); milling of cell residue, 1500 rpm, 10 min; Ag leaching with HNO_3 60 %, 25 °C, stirring at 180 rpm

hydrometallurgical steps, based on leaching, precipitation and electrowinning. Applied to already liberated fractions, these steps recover silver up to 99.99 % [79], silicon up to 4N (99.99 %) [84] and copper above 99 % [88], while aluminium is recovered as high-purity alumina [82]. In line with this, the high-value recovery of silicon, rather than of intact wafers, has been identified as the more promising target, provided that contaminants are identified and a dedicated purification is applied [104].

Rather than a standalone alternative, these chemical steps typically act as the refining stage that follows the mechanical and, in many plants, thermal pre-treatment. It is therefore the integrated routes, combining mechanical, thermal and chemical operations, that report the highest purities so far achieved on real EoL modules. At pilot and industrial scale, the PHOTORAMA process recovers silicon at 5N and silver above 2N, the ROSI process recovers silicon at 3 to 5N (99.9 to 99.999 %), and the 9-Tech pilot recovers silicon and copper at about 95 % purity and silver up to 95 % [101,103]. The FRELP process recovers all the main fractions, glass, aluminium, copper and silver, with silicon obtained at metallurgical grade and destined for further purification [105]. The high nominal purities reported for the single chemical steps in laboratory studies are obtained on pre-selected fractions and at small scale, whereas the integrated plants reach comparable purities on the whole module, with the losses and cross-contamination of the real waste stream. The purity reached in turn governs the destination of each fraction, with silicon directed to foundry and metallurgical uses or, once purified, to battery anodes and sputter targets, the non-ferrous metals sent to

smelters and refineries, and the recovered glass re-entering flat-glass production [101]. The remaining limitation, as the surveys repeatedly note, is the incomplete and non-harmonised reporting of purity, which still constrains a rigorous comparison across methods [101].

6. Discussion

The PV module recycling sector is currently in a critical transitional phase. On one hand, the scientific literature has produced a considerable body of studies over the past two decades demonstrating the technical feasibility of recovering the main constituent materials of the module; on the other hand, the vast majority of these processes remain confined to the laboratory scale, and the percentage of EoL modules actually recycled on an industrial scale remains very low globally [17,22,106]. Europe represents a significant exception in this context, thanks to the inclusion of PV modules in the WEEE Directive of 2012 and the introduction of binding collection and recycling obligations for producers, with specific targets that include recovering 85 % of collected PV panel waste and preparing for the reuse and recycling of 80 % by weight [107]. However, even within the European Union, the results remain uneven; in 2021, only 6 out of the 12 countries that reported data achieved these targets [107], and many treatment facilities still incinerate part of the mass of the panels, dispersing economically significant materials such as silver, copper, and silicon [107]. Outside of Europe, countries with high installed capacities still lack specific regulations for the management of PV modules, making landfill or uncontrolled disposal the predominant practice [1,5]. This disparity between scientific progress and industrial reality is not coincidental but reflects a series of structural issues that cut across all the recycling technologies discussed in the previous sections.

A primary fundamental issue concerns the toxicity of the reagents used in chemical delamination and hydrometallurgical recovery processes. Most metal leaching processes are based on nitric acid (HNO_3), which generates toxic NO_x fumes during the reaction [78], and on reagents such as hydrofluoric acid (HF), trichloroethylene, and toluene, which pose serious health risks to operators and the environment in case of dispersion [8,106]. The use of these reagents introduces significant additional costs related to emission abatement systems, wastewater treatment, and the necessary safety measures for their management, as well as generating a secondary environmental impact that in some cases can reduce or negate the environmental benefits of recycling compared to landfill disposal [106]. The trend towards more sustainable reagents, such as green solvents, DES, and ammoniacal systems, is promising but still far from industrial implementation, mainly due to longer processing times, higher costs, and lower scalability compared to conventional reagents [5,8,60].

A second structural criticality is represented by the compositional heterogeneity of PV modules. Although the general structure of c-Si modules is standardised, manufacturers employ different materials, thicknesses, metal contact compositions and backsheet typologies, and these differences have become more pronounced over the years with technological evolution [33]. In particular, the efficiency of metal recovery through chemical treatment strongly depends on the quantity and nature of the materials present in the cell, making the universal application of a single process protocol to modules from different manufacturers and years difficult [33]. This heterogeneity represents a significant obstacle to the development of standardised and scalable recycling processes, and requires adaptive approaches capable of managing heterogeneous input streams [5,23].

Closely related to this point is the issue of damaged modules: although a significant portion of the modules that reach the end of their life cycle exhibit mechanical damage such as glass breakage, frame deformation, or EVA degradation due to weather events, accidents during transport or installation, or structural failures, the literature has focused almost exclusively on the recycling of intact modules [14,64]. The treatment of broken or deformed modules poses specific challenges, as chemical delamination processes require longer times due to the lower uniformity of solvent exposure; moreover, methods based on hot knives or supercritical CO_2 are inapplicable in the presence of significant deformations. The development of robust processes for the treatment of heterogeneous input streams that include damaged modules is therefore a research priority that has not yet been adequately addressed [14]. Beyond adapting the recycling processes to this variability, a complementary approach acts upstream, on the modules themselves. Standardising module design, in particular physical dimensions such as frame size, has been argued to enable more efficient disassembly, material recovery and reuse of components, supported by policy instruments such as extended producer responsibility [108].

A third critical aspect concerns the gap between laboratory scale and industrial scale. Almost all the studies analysed in this review were conducted on small-sized samples, typically module fragments of a few square decimetres or portions equivalent to a single cell, under optimised operating conditions that do not replicate the variability and complexity of a continuous industrial process [12,17]. The transition to industrial scale introduces heat and mass transfer problems that significantly alter the efficiency of thermal and chemical processes, requires engineering solutions for the management of wastewater and emissions on much larger volumes, and imposes stringent economic constraints related to the investment and operating costs of the plants [17]. Emblematic in this sense is the case of the ReSiELP process, one of the most recent examples of silicon upcycling at the pilot scale, which, despite demonstrating the technical feasibility of the process, proved unprofitable in its demonstration phase mainly due to the energy costs of the furnace (€460/ton), the large amount of wastewater generated (€550/ton), and the high labour demand for non-automated operations (€1700/ton) [17]. These data illustrate how the optimised laboratory conditions are hardly directly transposable to the industrial scale without significant process engineering work.

This gap takes on particular significance in light of projections regarding PV waste flows in the coming years, when the modules installed during the first major expansion cycle of the PV market, approximately between 2007 and 2012, will reach the end of their lifecycle [9,37]. The current flows of EoL PV modules are insufficient to economically justify investments in high-capacity recycling plants [9]. However, the concrete risk is that when waste flows become sufficiently consistent to make large-scale recycling economically viable, the available technologies may not yet be mature enough to handle them effectively [8].

This urgent scenario contrasts with a structural aspect of the sector that deserves critical reflection, namely the disparity between investments in research and development aimed at improving the efficiency of PV modules and those dedicated to the development of recycling processes. The PV industry has historically focused its R&D resources on improving conversion efficiency and reducing production costs, while the development of economically advantageous strategies for the disassembly and recycling of EoL modules has received comparatively less attention. Research on recycling processes is also predominantly academic and focused on demonstrating technical feasibility, with limited attention to evaluating the economic and environmental sustainability on an industrial scale, a fundamental requirement that should accompany any new process proposal from the early stages of development [17,23].

A promising response to the scale-up and process-optimisation challenges outlined above is the recent application of computational modelling to PV recycling. This novel approach complements laboratory work by allowing the underlying processes to be analysed and optimised at the level of the individual particles. Two process stages have received particular attention. The first is the mechanical separation of the crushed module stream. Discrete element method (DEM) models reproduce the screening of the shape-diverse fragments produced when the module is crushed, such as rod-like glass particles, chip-like cell fragments and fine residues. They capture the looseness, stratification,

collision and penetration of the individual particles, quantify how the vibration parameters govern the separation efficiency and identify optimal operating conditions for device scale-up [109]. More advanced formulations represent the real, non-spherical particle shapes, as in the superquadric DEM used to design multi-deck vibrating screens for mixtures of markedly different particle shapes [110]. The second stage is the hydrometallurgical recovery of metals. Here, coupled computational fluid dynamics and discrete element method (CFD-DEM) models, combined with experimentally derived reaction kinetics, describe the reacting flow during silver leaching. At the particle scale, this approach explains why finer particles are leached more efficiently, by roughly a factor of 1.3 for the finest fraction [111]. At the reactor scale, the same modelling approach, validated against laboratory data, has been used to optimise a continuous stirred-tank reactor, showing that a modified impeller arrangement, with a lower position and additional impeller layers, improves the reactor hydrodynamics and the leaching performance [112]. Although still confined to the laboratory and modelling domain, these approaches are valuable. They reduce the empirical trial-and-error inherent in process development and offer a cost-effective route to the reliable scale-up that the sector currently lacks.

An additional limiting factor is represented by the logistical challenges of collecting and transporting EoL modules. Unlike other streams of electronic waste, PV modules are installed in geographically dispersed and often remote locations, residential rooftops, industrial plants, large PV parks in rural or high-altitude areas, making the collection and transportation to centralised recycling facilities particularly burdensome [8,9]. Life cycle assessment studies have shown that the costs and environmental impacts of transportation can represent a dominant component of the overall balance of the recycling process. For the FRELP process, transportation accounts for 29 % of the overall climate impact of the process [82], and the analysis by Lunardi et al. has shown that for distances greater than 80 km from the collection point to the recycling centre, the environmental benefits of recycling compared to landfill disposal or incineration are significantly reduced [106].

Finally, one last often-overlooked issue concerns the gap between the recovery yields reported in the literature and the actual marketability of the obtained materials. High yields do not guarantee that the recovered materials will meet the purity levels required by the relevant secondary markets. Thermal treatment, for example, typically leaves superficial metallic contaminations on the glass, making it unsuitable to produce new flat glass for PV applications, requiring further treatments or limiting its reuse to lower value-added applications [96]; in contrast, solar-grade glass has been recovered through chemical treatment [15]. In the absence of established secondary markets for recovered materials, these can turn from a source of income into an additional cost for the recycler. Glass, which despite representing 70–76 % of the module's mass has a very low market value, is the most emblematic example [96,97]. The economic sustainability of recycling therefore depends not only on the technical efficiency of the process but also on the ability to place the recovered materials in production chains with purity and standardisation requirements compatible with the available recycling processes, creating a condition that requires collaboration between the photovoltaic recycling sector and the industries using secondary materials [23].

7. Life cycle assessment of the recycling routes

Life cycle assessment (LCA) evaluates the potential environmental impacts of a product or process over its entire life cycle and has become a key tool for assessing the EoL management of c-Si PV modules [113]. Its benefit for recycling arises mainly from the avoided production of the virgin materials and energy that the recovered fractions displace [106,113]. LCA studies typically compare three scenarios, namely landfilling, downcycling and upcycling. Across these studies upcycling yields the greatest environmental benefit, downcycling an intermediate one, and landfilling the worst, the combination of incineration and landfilling being the least favourable option [114,115]. The same pattern holds at the process level for a laser-based recycling route, where the full recovery of aluminium, silicon, glass and silver chloride yields about 84 % greater environmental benefit than a partial recovery limited to the bulk fractions [116]. The absolute results differ widely between studies, with reported differences of up to about 99.86 % for the same scenario, owing to differences in functional units, system boundaries and assumed electricity mixes, which limits their direct comparability and calls for caution in their interpretation [113].

Contribution and sensitivity analyses consistently identify the same environmental hotspots, namely the thermal (incineration) steps, the electricity consumed by the process and the transportation of the modules to the recycling plant [117]. The electricity mix is particularly decisive, the substitution of grid power by renewable electricity increasing the environmental benefit of recycling by a factor of five, while the transportation distance alone can shift the climate-change and resource-scarcity impacts by 10 to 16 % [27,118]; because transportation is so influential, mobile or on-site recycling plants have been proposed to reduce it [119]. A comparative LCA of the main routes, moreover, found that each achieves the best net performance on a different impact category, mechanical recycling on life-cycle energy use, chemical recycling on water consumption and thermal recycling on global warming potential, once the credits for the recovered materials and energy are taken into account, so that no single route is environmentally optimal across all categories [120]. The net outcome of the more energy-intensive routes such as pyrolysis therefore depends strongly on the electricity mix and on the credits assigned to the recovered materials, consistent with the trade-offs discussed for the individual delamination routes.

For the perspective adopted in this review, the most relevant conclusion of the LCA literature concerns the coupling between environmental and economic performance, the economic factor being widely regarded as the main obstacle to the development of the recycling industry [121].

The environmentally preferable option, upcycling, is at present the least economically attractive, whereas the mechanical downcycling that performs worse environmentally is more viable in economic terms, so that the two objectives currently point in opposite directions. Sensitivity analyses indicate that the revenue from silver, aluminium and silicon is the parameter that most strongly governs this economic viability [26], so that the environmental benefit of advanced recycling, although clear, will be realised at industrial scale only once the recovery of these high-value materials becomes profitable and low-carbon electricity is used [113]. It should finally be noted that most LCA studies to date have neglected the component-sorting steps and the recovery of the low-value fractions, a gap that future assessments will need to address [26].

8. Economic sustainability

The economic sustainability of PV module recycling represents the most decisive barrier to the transition towards a mature industrial system. Despite the quantitative estimates available in the literature varying considerably depending on the geographical context, model assumptions, and the process analysed, some structural trends emerge robustly.

Under current conditions, landfill disposal remains the most economically advantageous option for PV waste managers in the absence of regulatory constraints, as the costs of recycling processes systematically exceed the revenues from the sale of recovered materials [75,86,122–124]. The most critical factor for reversing this relationship is the volume of waste available for treatment. Only above certain capacity thresholds do economies of scale allow for the reduction of unit process costs to a level compatible with profitability. Such thresholds vary significantly depending on the process and the technological level of the plant. Cucchiella et al. reported that profitability is verified above

approximately 19,000 t/year, a threshold below which collection and processing costs exceed revenues even in the optimistic scenario [122]. For more complex processes, which integrate mechanical, chemical, and hydrometallurgical treatment for the recovery of silver and silicon, the thresholds are considerably higher. Rubino et al. demonstrated that the advanced PhotoLife process achieves profitability only at 30,000 t/year, with a payback period of approximately 3.5 years, while at 3000 t/year the same process generates operating costs more than double the revenues [125]. For a laser-based recycling process, the processing cost is higher than that of established routes, and the process becomes profitable only above a throughput that current laser equipment has not yet demonstrated. With labour and raw material dominating this cost, the route is not yet viable under present technical and market conditions [116]. Choi & Fthenakis, through an integrated reverse supply chain optimisation model applied to the German context, have shown that the optimal localisation of collection centres and the minimisation of logistics costs are equally decisive conditions for profitability as the volume processed, and that the collection component is the cost parameter to which the profitability of the recycler is most sensitive [126]. The achievement of the necessary capacity thresholds is nonetheless precluded under current conditions, where EoL waste flows are still insufficient, and it is expected that they will remain so at least until the expected peak in disposals around 2030–2035. Confirming the structural difficulty of the sector, c-Si modules stand out from other electronic waste streams due to a revenue potential per unit mass that is two orders of magnitude lower than products like smartphones or computers, making it structurally more difficult to economically justify the costs of collection and treatment [75].

The material composition of the modules directly determines this difficulty. Most of the mass is occupied by glass and aluminium, abundant and low-cost materials that, despite dominating the revenues in terms of quantity, are not sufficient to cover the processing costs in low-capacity systems. The economically most valuable components are present in small quantities but account for a high share of the total recoverable value. Silver, despite constituting less than 0.1 % of the module's mass, represents the main source of revenue in many upcycling processes, and its recovery yield proves to be the most sensitive economic parameter in the entire process balance [125,127]. This economic role of silver is, however, being eroded from the manufacturing side. Since silver is a major contributor to cell cost, the amount used per cell has been progressively reduced, so that modules reaching end of life in future will contain less silver and yield a lower recycling revenue [128]. This may be partly offset by the price of silver, because the reduction per cell has not kept pace with the growth of the photovoltaic industry, whose rising overall silver demand is expected to keep prices under upward pressure [128]. Silicon offers economic potential that is highly dependent on the form in which it is recovered. The value of intact solar-grade wafers is significantly higher than that of metallurgical-grade silicon powder, making processes capable of preserving the integrity of the wafers potentially much more profitable, provided that additional costs are contained [75,123]. This dependence on recovery quality is still insufficiently considered in economic models that tend to value materials at the price of the simplest form.

The logistics of collection and transportation constitute another significant cost component. Markert et al. quantified that process transportation constitutes the highest private cost item in the EoL management of the module, in the case of the FRELP process [127]. This result highlights how the geographical dispersion of PV plants makes the construction of efficient collection networks a necessary but costly condition for any economically sustainable recycling scheme [126,129]. The optimisation of collection routes and the proximity of treatment plants to installation areas are therefore systemic design elements as relevant as the technological aspects of the process. In this sense, solutions such as the reversal of the existing distribution network where the same installers act as collectors during module replacement, or digital platforms that connect waste producers and recyclers have been proposed as mechanisms to reduce logistical costs and increase collection rates [130].

The recycling of PV modules cannot become economically self-sufficient without an appropriate regulatory and incentive framework. Two policy levers emerge as particularly effective: the introduction of higher landfill fees or the ban on direct disposal, which reduces the competitive advantage of landfilling compared to recycling [75]; and extended producer responsibility (EPR) mechanisms, which transfer EoL management costs to producers, creating structural incentives for eco-design and funding the collection system [75,130]. The transition towards economically sustainable PV recycling on an industrial scale therefore requires a systemic approach that integrates technological innovation in recovery processes, the development of secondary markets for recovered materials, and the construction of efficient collection infrastructures [75,130].

9. Conclusions

Among the delamination processes, pyrolysis in an inert atmosphere remains the most thermally established technology, capable of removing over 99 % of the polymers present in the module at 500 °C for 30 min, although the generation of fluorinated by-products during the decomposition of backsheet requires dedicated abatement systems. The preventive mechanical removal of the backsheet before thermal treatment has proven to be an effective strategy to eliminate this problem, simultaneously reducing process times and the environmental impact of emissions. Chemical delamination processes with green solvents and deep eutectic solvents represent a promising research direction to overcome the toxicity of traditional organic reagents, although longer treatment times and higher costs still limit their industrial applicability. Advanced processes (laser irradiation, hydrodynamic fragmentation, supercritical CO_2, and treatments in a pressurised reactor) offer superior selectivity and quality of separated materials compared to conventional methods, but they remain predominantly confined to the laboratory scale.

Hydrometallurgy represents the dominant approach for the selective recovery of silicon, silver, aluminium, and copper, with high yields for precious metals under optimised conditions. Silicon constitutes the material of the highest strategic value, whose purification to solar-grade is a necessary condition for re-entry into the PV production chain. Silver, although present in amounts less than 0.1 % of the module's mass, represents the main source of revenue in upcycling processes and has received the most attention in the literature. Alternative leaching systems, such as ammoniacal solutions, peroxidic systems, and DES, show potential to reduce toxicity and effluent generation, but require further development to achieve the yields and scalability of conventional reagents.

The critical analysis of the sector highlights that the main obstacle to the industrial maturity of PV recycling is not technical but systemic. Almost all the processes proposed in the literature have been validated on a laboratory scale under optimised conditions that do not replicate the variability and complexity of a continuous industrial process. Life cycle assessment confirms that recycling is environmentally preferable to landfilling, chiefly through the burdens avoided by the recovered materials, yet no single route minimises all environmental impacts, and the net benefit depends strongly on the electricity mix and on the recovery of the high-value fractions, so that the environmentally preferable upcycling remains at present the least economically attractive. The economic sustainability of recycling is structurally conditioned by the volume of waste available, the quality and marketability of the recovered materials, and the logistical costs of collection and transportation, which in many contexts exceed the cost of the recycling process. In the absence of regulatory constraints, landfill disposal remains the most economically advantageous option, making a regulatory framework based on extended producer responsibility and adequate economic incentives indispensable.

The next decade will represent a critical turning point for the sector. The modules installed during the first expansion cycle of the photovoltaic market between 2007 and 2012 will reach the end of their nominal life cycle, generating unprecedented waste flows. The window of time available to develop mature processes, build efficient collection infrastructures, and define secondary markets for recovered materials is rapidly closing. Emerging tools such as particle-scale computational modelling of the separation and leaching steps offer a promising and cost-effective route to bridge the gap between laboratory results and reliable industrial scale-up. Addressing this challenge will require an integrated approach that combines technological innovation, regulatory development, and structured collaboration between the recycling sector and industries that use secondary materials.

Declaration of generative AI and AI-assisted technologies in the writing process

During the preparation of this work the author(s) used Claude (Anthropic) to improve the clarity and readability of the text. After using this tool, the author(s) reviewed and edited the content as needed and take(s) full responsibility for the content of the publication.

CRediT authorship contribution statement

Andrea Franzoni: Data curation, Methodology, Writing – original draft, Writing – review & editing. **Mariasole Bannò:** Supervision, Writing – review & editing. **Mattia Avanzini:** Methodology, Writing – original draft, Writing – review & editing.

Declaration of competing interest

The authors declare that they have no known competing financial interests or personal relationships that could have appeared to influence the work reported in this paper.

Data availability

Data will be made available on request.

References

[1] X. Li, H. Liu, J. You, H. Diao, L. Zhao, W. Wang, Back EVA recycling from c-Si photovoltaic module without damaging solar cell via laser irradiation followed by mechanical peeling, Waste Manag. 137 (2022) 312–318, https://doi.org/10.1016/j.wasman.2021.11.024.

[2] P.S.S. Camargo, A. da S. Domingues, J.P.G. Palomero, M.P. Cenci, A.C. Kasper, P. R. Dias, H.M. Veit, c-Si PV module recycling: analysis of the use of a mechanical pre-treatment to reduce the environmental impact of thermal treatment and enhance materials recovery, Waste Manage. Res. 41 (2023) 1661–1673, https://doi.org/10.1177/0734242X231166308.

[3] M. Niekurzak, W. Lewicki, H.H. Coban, A. Brelik, Conceptual design of a semi-automatic process line for recycling photovoltaic panels as a way to ecological sustainable production, Sustainability 15 (2023), https://doi.org/10.3390/su15032822.

[4] E. Klugmann-Radziemska, P. Ostrowski, K. Drabczyk, P. Panek, M. Szkodo, Experimental validation of crystalline silicon solar cells recycling by thermal and chemical methods, Sol. Energy Mater. Sol. Cell. 94 (2010) 2275–2282, https://doi.org/10.1016/j.solmat.2010.07.025.

[5] M. Wahman, A. Surowiak, Recycling of discarded photovoltaic modules using mechanical and thermal methods, Inzynieria Mineralna 1 (2022) 107–116, https://doi.org/10.29227/IM-2022-01-13.

[6] B. Jung, J. Park, D. Seo, N. Park, Sustainable system for raw-metal recovery from crystalline silicon solar panels: from noble-metal extraction to lead removal, ACS Sustain. Chem. Eng. 4 (2016) 4079–4083, https://doi.org/10.1021/acssuschemeng.6b00894.

[7] I. Riech, C. Castro-Montalvo, L. Wittersheim, G. Giácoman-Vallejos, A. González-Sánchez, C. Gamboa-Loira, M. Acosta, J. Méndez-Gamboa, Experimental methodology for the separation materials in the recycling process of silicon photovoltaic panels, Materials 14 (2021) 581, https://doi.org/10.3390/ma14030581.

[8] E. Klugmann-Radziemska, P. Ostrowski, Chemical treatment of crystalline silicon solar cells as a method of recovering pure silicon from photovoltaic modules, Renew. Energy 35 (2010) 1751–1759, https://doi.org/10.1016/j.renene.2009.11.031.

[9] P.J.M. Isherwood, Reshaping the module: the path to comprehensive photovoltaic panel recycling, Sustainability 14 (2022), https://doi.org/10.3390/su14031676.

[10] G. Granata, F. Pagnanelli, E. Moscardini, T. Havlik, L. Toro, Recycling of photovoltaic panels by physical operations, Sol. Energy Mater. Sol. Cell. 123 (2014) 239–248, https://doi.org/10.1016/j.solmat.2014.01.012.

[11] P. Dias, S. Javimczik, M. Benevit, H. Veit, A.M. Bernardes, Recycling WEEE: extraction and concentration of silver from waste crystalline silicon photovoltaic modules, Waste Manag. 57 (2016) 220–225, https://doi.org/10.1016/j.wasman.2016.03.016.

[12] J. wen Zhang, H. dong Wang, S. guang Zhang, H. Liang, H. Guo, S. yao Tao, Research on new process for separation of silicon wafers and glass from decommissioned photovoltaic modules, in: Physicochemical Problems of Mineral Processing, 58, 2022, https://doi.org/10.37190/ppmp/151679.

[13] IRENA and IEA-PVPS, End-Of-Life Management, Solar Photovoltaic Panels, 2016.

[14] D. Jiang, S. Qin, P. Li, S. Shi, S. Wen, Y. Tan, Electromagnetic separation of silicon carbide inclusions with aluminum penetration in silicon by imposition of supersonic frequency magnetic field, J. Clean. Prod. 145 (2017) 45–49, https://doi.org/10.1016/j.jclepro.2017.01.041.

[15] F. Pagnanelli, E. Moscardini, P. Altimari, F.C.S.M. Padoan, T. Abo Atia, F. Beolchini, A. Amato, L. Toro, Solvent versus thermal treatment for glass recovery from end of life photovoltaic panels: environmental and economic assessment, J. Environ. Manag. 248 (2019), https://doi.org/10.1016/j.jenvman.2019.109313.

[16] C.C. Farrell, A.I. Osman, R. Doherty, M. Saad, X. Zhang, A. Murphy, J. Harrison, A.S.M. Vennard, V. Kumaravel, A.H. Al-Muhtaseb, D.W. Rooney, Technical challenges and opportunities in realising a circular economy for waste photovoltaic modules, Renew. Sustain. Energy Rev. 128 (2020), https://doi.org/10.1016/j.rser.2020.109911.

[17] F. Ardente, C.E.L. Latunussa, G.A. Blengini, Resource efficient recovery of critical and precious metals from waste silicon PV panel recycling, Waste Manag. 91 (2019) 156–167, https://doi.org/10.1016/j.wasman.2019.04.059.

[18] Y. Kim, J. Lee, Dissolution of ethylene vinyl acetate in crystalline silicon PV modules using ultrasonic irradiation and organic solvent, Sol. Energy Mater. Sol. Cell. 98 (2012) 317–322, https://doi.org/10.1016/j.solmat.2011.11.022.

[19] S. He, K. Zhang, W. Zhang, P. Deng, J. Li, X. Xie, Y. Han, D. Qin, X. Wang, L. Lin, Effectively and completely separating the waste crystalline silicon photovoltaic modules via green solvothermal strategy, Sep. Purif. Technol. 359 (2025) 130682, https://doi.org/10.1016/j.seppur.2024.130682.

[20] P. Dias, L. Schmidt, L.B. Gomes, A. Bettanin, H. Veit, A.M. Bernardes, Recycling waste crystalline silicon photovoltaic modules by electrostatic separation, J. Sustain. Metall. 4 (2018) 176–186, https://doi.org/10.1007/s40831-018-0173-5.

[21] J. Wang, Y. Feng, Y. He, The research progress on recycling and resource utilization of waste crystalline silicon photovoltaic modules, Sol. Energy Mater. Sol. Cell. 270 (2024) 112804, https://doi.org/10.1016/j.solmat.2024.112804.

[22] V. Savvilotidou, E. Gidarakos, Pre-concentration and recovery of silver and indium from crystalline silicon and copper indium selenide photovoltaic panels, J. Clean. Prod. 250 (2020), https://doi.org/10.1016/j.jclepro.2019.119440.

[23] P.R. Dias, M.G. Benevit, H.M. Veit, Photovoltaic solar panels of crystalline silicon: characterization and separation, Waste Manage. Res. 34 (2016) 235–245, https://doi.org/10.1177/0734242X15622812.

[24] R. Sanathi, S. Banerjee, S. Bhowmik, A technical review of crystalline silicon photovoltaic module recycling, Sol. Energy 281 (2024) 112869, https://doi.org/10.1016/j.solener.2024.112869.

[25] O. Celep, H. Deveci, E.Y. Yazici, A comprehensive review on recycling end of life solar photovoltaic panels, Waste Manag. 206 (2025) 115092, https://doi.org/10.1016/j.wasman.2025.115092.

[26] P. Su, Y. He, Y. Feng, Q. Wan, T. Li, Advancements in end-of-life crystalline silicon photovoltaic module recycling: current state and future prospects, Sol. Energy Mater. Sol. Cell. 277 (2024) 113109, https://doi.org/10.1016/j.solmat.2024.113109.

[27] P.R. Dias, L. Schmidt, N.L. Chang, M. Monteiro Lunardi, R. Deng, B. Trigger, L. Bonan Gomes, R. Egan, H. Veit, High yield, low cost, environmentally friendly process to recycle silicon solar panels: technical, economic and environmental feasibility assessment, Renew. Sustain. Energy Rev. 169 (2022), https://doi.org/10.1016/j.rser.2022.112900.

[28] T. Dobra, D. Vollprecht, R. Pomberger, Thermal delamination of end-of-life crystalline silicon photovoltaic modules, Waste Manage. Res. 40 (2022) 96–103, https://doi.org/10.1177/0734242X211038184.

[29] S. Lim, Y. Imaizumi, K. Mochidzuki, T. Koita, T. Namihira, C. Tokoro, Recovery of silver from waste crystalline silicon photovoltaic cells by wire explosion, IEEE Trans. Plasma Sci. 49 (2021) 2857–2865, https://doi.org/10.1109/TPS.2021.3106307.

[30] Y.K. Yi, H.S. Kim, T. Tran, S.K. Hong, M.J. Kim, Recovering valuable metals from recycled photovoltaic modules, J. Air Waste Manage. Assoc. 64 (2014) 797–807, https://doi.org/10.1080/10962247.2014.891540.

[31] M. Tammaro, J. Rimauro, V. Fiandra, A. Salluzzo, Thermal treatment of waste photovoltaic module for recovery and recycling: experimental assessment of the presence of metals in the gas emissions and in the ashes, Renew. Energy 81 (2015) 103–112, https://doi.org/10.1016/j.renene.2015.03.014.

[32] J. Li, S. Yan, Y. Li, Z. Wang, Y. Tan, J. Li, M. Xia, P. Li, Recycling Si in waste crystalline silicon photovoltaic panels after mechanical crushing by electrostatic

separation, J. Clean. Prod. 415 (2023), https://doi.org/10.1016/j.jclepro.2023.137908.
[33] P. Su, Y. He, S. Nazari, Y. Feng, N. Wei, J. Wang, J. Li, Y. Liu, Environmentally friendly recycling process for crystalline silicon photovoltaic modules: airflow separation and AlCl3·6H2O + H2O2 etching system, Sep. Purif. Technol. 343 (2024), https://doi.org/10.1016/j.seppur.2024.127043.
[34] T. Doi, I. Tsuda, H. Unagida, A. Murata, K. Sakuta, K. Kurokawa, Experimental Study on PV Module Recycling with Organic Solvent Method, 2001.
[35] D.S. Prasad, B. Sanjana, D.S. Kiran, P.P. Srinivasa Kumar, R. Ratheesh, Process optimization studies of essential parameters in the organic solvent method for the recycling of waste crystalline silicon photovoltaic modules, Sol. Energy Mater. Sol. Cell. 245 (2022), https://doi.org/10.1016/j.solmat.2022.111850.
[36] Y. Yan, Z. Wang, D. Wang, J. Cao, W. Ma, K. Wei, L. Yun, Recovery of silicon via using KOH-ethanol solution by separating different layers of end-of-life PV modules, JOM 72 (2020) 2624–2632, https://doi.org/10.1007/s11837-020-04193-6.
[37] Z. Zhang, M. Liu, L. Wang, T. Chen, L. Zhao, Y. Hu, C. Xu, Optimization of indium recovery from waste crystalline silicon heterojunction solar cells by acid leaching, Sol. Energy Mater. Sol. Cell. 230 (2021), https://doi.org/10.1016/j.solmat.2021.111218.
[38] M. Luo, F. Liu, Z. Zhou, L. Jiang, M. Jia, Y. Lai, J. Li, Z. Zhang, A comprehensive hydrometallurgical recycling approach for the environmental impact mitigation of EoL solar cells, J. Environ. Chem. Eng. 9 (2021), https://doi.org/10.1016/j.jece.2021.106830.
[39] J. Vaněk, K. Jandova, P. Vanýsek, P. Maule, Chemical delamination applicable to a low-energy recycling process of photovoltaic modules, Processes 11 (2023), https://doi.org/10.3390/pr11113078.
[40] P. Dias, S. Javimczik, M. Benevit, H. Veit, Recycling WEEE: polymer characterization and pyrolysis study for waste of crystalline silicon photovoltaic modules, Waste Manag. 60 (2017) 716–722, https://doi.org/10.1016/j.wasman.2016.08.036.
[41] M. Huang, Q. Song, Y. Wang, Y. Liu, Z. Xu, Thermostatic pyrolysis decapsulation and pollution control of waste crystalline silicon photovoltaic panels: kinetic analysis and organics evolution, Sol. Energy 300 (2025) 113765, https://doi.org/10.1016/j.solener.2025.113765.
[42] P.S.S. Camargo, A. da S. Domingues, J.P.G. Palomero, A.C. Kasper, P.R. Dias, H. M. Veit, Photovoltaic module recycling: thermal treatment to degrade polymers and concentrate valuable metals, Detritus 16 (2021) 48–62, https://doi.org/10.31025/2611-4135/2021.15119.
[43] R. Wang, E. Song, C. Zhang, X. Zhuang, E. Ma, J. Bai, W. Yuan, J. Wang, Pyrolysis-based separation mechanism for waste crystalline silicon photovoltaic modules by a two-stage heating treatment, RSC Adv. 9 (2019) 18115–18123, https://doi.org/10.1039/c9ra03582f.
[44] V. Fiandra, L. Sannino, C. Andreozzi, G. Graditi, End-of-life of silicon PV panels: a sustainable materials recovery process, Waste Manag. 84 (2019) 91–101, https://doi.org/10.1016/j.wasman.2018.11.035.
[45] M. Królikowski, M. Fotek, P. Żach, M. Michałowski, Development of a recycling process and characterization of EVA, PVDF, and PET polymers from end-of-life PV modules, Materials 17 (2024), https://doi.org/10.3390/ma17040821.
[46] Z. Wu, S. Wang, D. Gao, X. Wei, C. Du, Z. Qi, A novel method for layer separation in waste crystalline silicon PV modules via combined low-temperature and thermal treatment, Waste Manag. 172 (2023) 299–307, https://doi.org/10.1016/j.wasman.2023.10.036.
[47] R.B.J. Salazar, J.A.S. Tenório, D.C.R. Espinosa, M. dos Passos Galluzzi Baltazar, Streamlined process with a sustainable approach for photovoltaic module recycling, Sustain. Mater. Technol. 41 (2024) e01047, https://doi.org/10.1016/j.susmat.2024.e01047.
[48] M.F. Azeumo, C. Germana, N.M. Ippolito, M. Franco, P. Luigi, S. Settimio, Photovoltaic module recycling, a physical and a chemical recovery process, Sol. Energy Mater. Sol. Cell. 193 (2019) 314–319, https://doi.org/10.1016/j.solmat.2019.01.035.
[49] J. Ko, K. Kim, J.W. Sohn, H. Jang, H.-S. Lee, D. Kim, Y. Kang, Review on separation processes of end-of-life silicon photovoltaic modules, Energies 16 (2023) 4327, https://doi.org/10.3390/en16114327.
[50] A. Ali, M. Shahid, S.A. Qadir, M.T. Islam, M.W. Khan, S. Ahmed, Solar PV end-of-life waste recycling: an assessment of mechanical recycling methods and proposed hybrid laser and high voltage pulse crushing method, Resources 13 (2024) 169, https://doi.org/10.3390/resources13120169.
[51] Y.R. Smith, J.R. Nagel, R.K. Rajamani, Electrodynamic eddy current separation of end-of-life PV materials, 379–386, https://doi.org/10.1007/978-3-319-52192-3_37, 2017.
[52] X. Wang, X. Tian, X. Chen, L. Ren, C. Geng, A review of end-of-life crystalline silicon solar photovoltaic panel recycling technology, Sol. Energy Mater. Sol. Cell. 248 (2022), https://doi.org/10.1016/j.solmat.2022.111976.
[53] M.M. Lunardi, J.P. Alvarez-Gaitan, J.I. Bilbao, R. Corkish, A review of recycling processes for photovoltaic modules, in: Solar Panels and Photovoltaic Materials, InTech, 2018, https://doi.org/10.5772/intechopen.74390.
[54] R. Frischknecht, K. Komoto, T. Doi, Life Cycle Assessment of Crystalline Silicon Photovoltaic Module Delamination with Hot Knife Technology, in: IEA PVPS Task 12, 12, International Energy Agency (IEA) PVPS Task, 2023. Report T12-25:2023, www.iea-pvps.org.
[55] Y. Takaya, Y. Imaizumi, T. Koita, C.U.E. Mauricio, C. Tokoro, Effect of electric pulse treatment on silver recovery from spent solar panel sheet by acid-leaching, J. Mater. Cycles Waste Manag. 26 (2024) 2591–2598, https://doi.org/10.1007/s10163-024-01951-5.
[56] S. Preet, S.T. Smith, A comprehensive review on the recycling technology of silicon based photovoltaic solar panels: challenges and future outlook, J. Clean. Prod. 448 (2024), https://doi.org/10.1016/j.jclepro.2024.141661.
[57] D. Sah Chitra, P. Saini, S. Kumar, Recovery and analysis of polymeric layers from waste solar modules by chemical route, Sol. Energy 244 (2022) 31–39, https://doi.org/10.1016/j.solener.2022.08.033.
[58] C. Wang, C. Pang, J. Lu, J. Zhu, J. Ruan, P-Toluene sulfonic acid and H2O2 synergistically strengthen terpinolene for efficient decapsulation of waste crystalline silicon photovoltaic laminates, Chem. Eng. J. 524 (2025) 169185, https://doi.org/10.1016/j.cej.2025.169185.
[59] G.H. Brenes, I. Riech, G. Giácoman-Vallejos, A. González-Sánchez, V. Rejón, Chemical method for ethyl vinyl acetate removal in crystalline silicon photovoltaic modules, Sol. Energy 263 (2023), https://doi.org/10.1016/j.solener.2023.05.055.
[60] P. Chowdhury, T. Chowdhury, P. Das, H. Chowdhury, E. Bontempi, R. Corkish, Green solvents for end-of-life photovoltaic module recycling: mechanisms, applications, environmental and economic perspectives, Sol. Energy Mater. Sol. Cell. 295 (2026) 113964, https://doi.org/10.1016/j.solmat.2025.113964.
[61] R. Min, W. Deng, Z. Wang, T. Qi, Z. Zhang, W. Xiao, G. Qian, D. Wang, Effective decapsulation method for photovoltaic modules: limonene-induced EVA controlled swelling under sonication and debonding mechanism analysis, J. Clean. Prod. 450 (2024), https://doi.org/10.1016/j.jclepro.2024.141917.
[62] C. Li, L. Zhao, F. Guo, X. Jiang, Y. Duan, W. Xu, Study on the separation of crystalline silicon photovoltaic modules using the green solvent NMP, Sol. Energy 293 (2025) 113453, https://doi.org/10.1016/j.solener.2025.113453.
[63] J. Lu, C. Wang, J. Zhu, Y. Wu, J. Ruan, Delamination of components for recovery of waste crystalline photovoltaic modules by three-step treatments of separating fluorinated coating, heating and ultrasonication, Chem. Eng. J. 506 (2025) 160335, https://doi.org/10.1016/j.cej.2025.160335.
[64] K. Li, Z. Wang, C. Liu, D. Wang, G. Li, X. Chen, G. Qian, K. Hu, A green method to separate different layers in photovoltaic modules by using DMPU as a separation agent, Sol. Energy Mater. Sol. Cell. 245 (2022), https://doi.org/10.1016/j.solmat.2022.111870.
[65] J. Lu, C. Wang, Y. Wu, J. Zhu, J. Ruan, Recycling of waste crystalline silicon photovoltaic modules: efficient decapsulation and silver extraction using environmental-friendly reagents and deep eutectic solvents, Sol. Energy Mater. Sol. Cell. 293 (2025) 113882, https://doi.org/10.1016/j.solmat.2025.113882.
[66] Y. Yu, J. Shi, X. Bai, Z. Zhang, F. Xi, S. Li, J. Lu, W. Ma, R. Deng, Green recycling of end-of-life photovoltaic modules via deep-eutectic solvents – part B, Chem. Eng. J. 512 (2025) 162345, https://doi.org/10.1016/j.cej.2025.162345.
[67] B.-T. Yang, Y.-H. Huang, C.-C. Chen, Hydrophobic deep eutectic solvents as novel media for the recycling of waste photovoltaic modules, Chem. Eng. J. 498 (2024) 155011, https://doi.org/10.1016/j.cej.2024.155011.
[68] T. Bin Anwar, K.M. Hanson, K. Lam, C.J. Bardeen, Using nanosecond laser pulses to debond the glass-EVA layer from silicon photovoltaic modules, Waste Manag. 187 (2024) 275–284, https://doi.org/10.1016/j.wasman.2024.07.013.
[69] P. Padhamnath, S. Nalluri, F. Kuśmierczyk, M. Kopyściański, J. Karbowniczek, S. W. Leow, T. Reindl, Electrohydraulic fragmentation processing enabling separation and recovery of all components in end-of-life silicon photovoltaic panels, Sol. Energy 289 (2025) 113329, https://doi.org/10.1016/j.solener.2025.113329.
[70] P. Padhamnath, S. Nalluri, F. Kuśmierczyk, M. Kopyściański, J. Karbowniczek, T. Kozieł, S.W. Leow, T. Reindl, Development of PV panel recycling process enabling complete recyclability of end-of-life silicon photovoltaic panels, Sol. Energy Mater. Sol. Cell. 286 (2025) 113571, https://doi.org/10.1016/j.solmat.2025.113571.
[71] A. Briand, A. Leybros, O. Doucet, J.C. Ruiz, P. Fontaine-Giraud, L. Liotaud, A. Grandjean, Versatility assessment of supercritical CO2 delamination for photovoltaic modules with ethylene-vinyl acetate, polyolefin or ethylene methacrylic acid ionomer as encapsulating polymer, J. Clean. Prod. 410 (2023), https://doi.org/10.1016/j.jclepro.2023.137292.
[72] A. Birtürk, M.S. Celiktas, Subcritical water delamination: a promising path to efficient recycling of critical minerals, J. Clean. Prod. 469 (2024) 143147, https://doi.org/10.1016/j.jclepro.2024.143147.
[73] K. Zhang, S. He, D. Qin, X. Xie, W. Zhang, P. Deng, J. Li, H. Rao, H. Deng, T. Mei, X. Wang, L. Lin, Green solvent hydrothermal recycling of end-of-life crystalline silicon photovoltaic modules, Chem. Eng. J. 515 (2025) 163759, https://doi.org/10.1016/j.cej.2025.163759.
[74] J. Park, N. Park, Wet etching processes for recycling crystalline silicon solar cells from end-of-life photovoltaic modules, RSC Adv. 4 (2014) 34823–34829, https://doi.org/10.1039/c4ra03895a.
[75] R. Deng, N.L. Chang, Z. Ouyang, C.M. Chong, A techno-economic review of silicon photovoltaic module recycling, Renew. Sustain. Energy Rev. 109 (2019) 532–550, https://doi.org/10.1016/j.rser.2019.04.020.
[76] W.S. Chen, Y.J. Chen, C.H. Lee, Y.J. Cheng, Y.A. Chen, F.W. Liu, Y.C. Wang, Y. L. Chueh, Recovery of valuable materials from the waste crystalline-silicon photovoltaic cell and ribbon, Processes 9 (2021), https://doi.org/10.3390/pr9040712.
[77] M. Theocharis, C. Pavlopoulos, P. Kousi, A. Hatzikioseyian, I. Zarkadas, P. E. Tsakiridis, E. Remoundaki, L. Zoumboulakis, G. Lyberatos, An Integrated Thermal and Hydrometallurgical Process for the Recovery of Silicon and Silver from End-of-Life Crystalline Si Photovoltaic Panels, Waste Biomass Valoriz. 13 (2022) 4027–4041, https://doi.org/10.1007/s12649-022-01754-5.
[78] A.R. Zubas, E. Griškonis, G. Denafas, V. Makarevičius, R. Kriūkienė, J. Kruopienė, NOx-Free leaching methods for efficient silver and aluminium recovery from

crystalline silicon solar cells, Materials 18 (2025) 2668, https://doi.org/10.3390/ma18112668.
[79] Y. Chen, T. Hu, X. Wang, X. Wang, Z. Wang, L. Zhang, S. Guan, T. Zhang, Z. Bian, Highly Selective Recovery of Silver from end-of-life Photovoltaic Panels, 31, Transactions of Tianjin University, 2025, pp. 452–462, https://doi.org/10.1007/s12209-025-00453-1.
[80] R. Zheng, M. Luo, B. Li, M. Jia, H. Zhang, S. Liu, Y. Lu, L. Jiang, Z. Zhang, F. Liu, Eco-friendly recovery and preparation of high purity nano silver powders from retired photovoltaic solar cells, Sep. Purif. Technol. 359 (2025) 130343, https://doi.org/10.1016/j.seppur.2024.130343.
[81] R. Yang, N. Zhu, Y. Xi, S. Gao, P. Wu, Z. Dang, Recovery of crystalline silicon from waste solar cells by a green deep eutectic solvent-hydrogen peroxide system, Green Chem. 26 (2024) 7246–7257, https://doi.org/10.1039/d4gc01322k.
[82] E. Kastanaki, E. Lagoudakis, G. Kalogerakis, A. Giannis, Hydrothermal leaching of silver and aluminum from waste monocrystalline and polycrystalline photovoltaic panels, Appl. Sci. 13 (2023), https://doi.org/10.3390/app13063602.
[83] S. Choi, H. Kang, E. Park, J. Yang, A. Gomez-Flores, H.J. Jung, S.W. Heo, J.-H. Lee, H. Jung, H. Kim, Pulse laser recovery of high-purity colloidal silver spheres from end-of-life crystalline silicon solar panels, Sep. Purif. Technol. 379 (2025) 134842, https://doi.org/10.1016/j.seppur.2025.134842.
[84] Y. Wang, C. Zhu, J. Qiu, W. Li, H. Wang, J. Yang, P. Shi, Y. Liu, A unique two-step process combining acid and alkaline etching for recovering high-purity silicon from waste crystalline silicon solar panels, Phys. Status Solidi 222 (2025), https://doi.org/10.1002/pssa.202400961.
[85] W.S. Chen, Y.J. Chen, K.C. Yueh, C.P. Cheng, T.C. Chang, Recovery of valuable metal from photovoltaic solar cells through extraction, in: IOP Conf. Ser. Mater. Sci. Eng., Institute of Physics Publishing, 2020, https://doi.org/10.1088/1757-899X/720/1/012007.
[86] D. Sah, S. Kumar, Experimental, cost and waste analysis of recycling process for crystalline silicon solar module, Sol. Energy 273 (2024), https://doi.org/10.1016/j.solener.2024.112534.
[87] B.N. Alsulami, J. Harwell, G. Zante, A.P. Abbott, A. Feeney, J. Kettle, Hybrid delamination of silver contacts from c-Si solar cells: a low environmental impact recycling approach, Resour. Conserv. Recycl. 221 (2025) 108429, https://doi.org/10.1016/j.resconrec.2025.108429.
[88] M. Kavousi, E.K. Alamdari, A comprehensive and sustainable recycling process for different types of blended end-of-life solar panels: leaching and recovery of valuable base and precious metals and/or elements, Metals 13 (2023), https://doi.org/10.3390/met13101677.
[89] M. Lin, P. Wang, B. Qin, J. Ruan, A novel acid-free combined technology to achieve the full recovery of crystalline silicon photovoltaic waste, Waste Manag. 190 (2024) 666–675, https://doi.org/10.1016/j.wasman.2024.10.031.
[90] E. Radziemska, T. Seramak, P. Ostrowski, Pure silicon recovering from photovoltaic modules, Adv. Mater. Sci. 8 (2009), https://doi.org/10.2478/v10077-008-0048-8.
[91] F. Chen, Y. Yang, M. Zhou, X. Huang, Y. Gao, K. Li, Z. Chen, C. Zhou, Z. Zhou, C. Zheng, X. Gao, Short process recovery of silver and purification mechanism of crystalline silicon deep etching from end-of-life photovoltaic cells, Chem. Eng. J. 510 (2025) 161651, https://doi.org/10.1016/j.cej.2025.161651.
[92] M.D. Rao, R. Singla, R.B. Meshram, Recycling of silicon and silver from end-of-life crystalline-Si solar PV cells, Can. Metall. Q. (2025) 1–12, https://doi.org/10.1080/00084433.2025.2569224.
[93] C. Liu, B. Lee, Recovery of complete crystalline silicon cells from waste crystalline silicon photovoltaic modules, J. Air Waste Manage. Assoc. 75 (2025) 735–745, https://doi.org/10.1080/10962247.2025.2513942.
[94] S. Rout, P. Jana, C.R. Borra, M.A.R. Önal, Unlocking silver from end-of-life photovoltaic panels: a concise review, Renew. Sustain. Energy Rev. 210 (2025) 115205, https://doi.org/10.1016/j.rser.2024.115205.
[95] P. Chowdhury, P. Das, H. Chowdhury, T. Chowdhury, E. Bontempi, R. Corkish, Assessing tin demand and supply pressures under terawatt-scale photovoltaic deployment, RSC Sustain. 4 (2026) 1581–1592, https://doi.org/10.1039/D5SU00956A.
[96] Y. Sim, Y.B. Tay, Ankit, X. Lin, N. Mathews, Simplified silicon recovery from photovoltaic waste enables high performance, sustainable lithium-ion batteries, Sol. Energy Mater. Sol. Cell. 257 (2023), https://doi.org/10.1016/j.solmat.2023.112394.
[97] P. Su, Y. He, J. Wang, Y. Feng, Q. Wan, Y. Zhang, Z. Pang, Green separation and decomposition of crystalline silicon photovoltaic module's backsheet by using ethanol, Waste Manag. 179 (2024) 144–153, https://doi.org/10.1016/j.wasman.2024.03.001.
[98] T. Chowdhury, M. Dehghanimadvar, N.L. Chang, R. Corkish, Review of issues and opportunities for glass supply for photovoltaic production at multiterawatt (TW) scale, Sustain. Energy Fuels 9 (2025) 1414–1431, https://doi.org/10.1039/D4SE01567C.
[99] T. Chowdhury, M. Dehghanimadvar, N.L. Chang, R. Corkish, Evaluating short-circularity pathways for photovoltaic glass through life cycle assessment: cullet recycling versus whole-glass reuse, Sol. Energy Mater. Sol. Cell. 300 (2026) 114227, https://doi.org/10.1016/j.solmat.2026.114227.
[100] P. Chowdhury, T. Chowdhury, H. Chowdhury, R. Corkish, N.L. Chang, Necessity for recycling photovoltaic glass: managing resource constraints and environmental impacts of antimony in terawatt scale photovoltaics, Sol. Energy Mater. Sol. Cell. 295 (2026) 114012, https://doi.org/10.1016/j.solmat.2025.114012.
[101] K. Wambach, C. Libby, Advances in photovoltaic module recycling: third update to empirical life cycle inventory data. https://doi.org/10.69766/PJOW5359, 2026.
[102] P.V.P.S. IEA, Status of PV Module Recycling in Selected IEA PVPS Task12 Countries 2022 PVPS Task 12 PV Sustainability, 2022. www.iea-pvps.org.
[103] K. Komoto, C. Agraffeil, C. Alonso-Garcia, D. Costa, T. Curtis, A. Danelli, R. Deng, N. Defrenne, K. Drozdiak, B. Ebin, N. Espinosa, A. Gassner, G. Heath, M. Held, J.-S. Lee, C. Libby, F. Lyu, H. Mirletz, M. Penn, Y. Shen, L. Smith, M. Stucki, M. Tammaro, M. Theelen, M. Vogt, C. Wessendorf, R. Woods-Robinson, Status of PV Module Recycling in IEA PVPS Task 12 Countries, 2025, https://doi.org/10.69766/XLFG7020.
[104] G.A. Heath, T.J. Silverman, M. Kempe, M. Deceglie, D. Ravikumar, T. Remo, H. Cui, P. Sinha, C. Libby, S. Shaw, K. Komoto, K. Wambach, E. Butler, T. Barnes, A. Wade, Research and development priorities for silicon photovoltaic module recycling to support a circular economy, Nat. Energy 5 (2020) 502–510, https://doi.org/10.1038/s41560-020-0645-2.
[105] C.E.L. Latunussa, F. Ardente, G.A. Blengini, L. Mancini, Life cycle assessment of an innovative recycling process for crystalline silicon photovoltaic panels, Sol. Energy Mater. Sol. Cell. 156 (2016) 101–111, https://doi.org/10.1016/j.solmat.2016.03.020.
[106] M.M. Lunardi, J.P. Alvarez-Gaitan, J.I. Bilbao, R. Corkish, Comparative life cycle assessment of end-of-life silicon solar photovoltaic modules, Appl. Sci. 8 (2018) 1396, https://doi.org/10.3390/app8081396.
[107] E.E.A. EEA, Recycling Materials from Green Energy Technologies, 2025.
[108] P. Chowdhury, H. Chowdhury, T. Chowdhury, R. Corkish, Standardization as a pathway to a circular PV industry: addressing material recovery and design challenges, Sol. Energy Mater. Sol. Cell. 296 (2026) 114067, https://doi.org/10.1016/j.solmat.2025.114067.
[109] X. Jin, Y. Zhuo, C. He, Z. Xie, Y. Shen, Design and optimisation of rotary vibrating screening process in silicon photovoltaic panel recycling: a particle-scale model study, Powder Technol. 440 (2024) 119787, https://doi.org/10.1016/j.powtec.2024.119787.
[110] H. Chowdhury, Z. Xie, Y. Shen, Superquadric DEM study of the particle separation process in a multi-deck banana vibrating screen, Adv. Powder Technol. 36 (2025) 105003, https://doi.org/10.1016/j.apt.2025.105003.
[111] S. Song, C. He, Y. Zhuo, Y. Yue, Y. Shen, How particle sizes affect silver leaching from c-Si photovoltaic solar cells: insights from integrated experimental and numerical investigations, Sol. Energy Mater. Sol. Cell. 261 (2023) 112520, https://doi.org/10.1016/j.solmat.2023.112520.
[112] S. Song, Y. Zhuo, Q. Li, Y. Shen, Silver recovery from crystalline silicon photovoltaic solar cells using continuous stirred-tank reactors, Adv. Mater. (2024), https://doi.org/10.1002/adma.202403653.
[113] D. Mao, S. Yang, L. Ma, W. Ma, Z. Yu, F. Xi, J. Yu, Overview of life cycle assessment of recycling end-of-life photovoltaic panels: a case study of crystalline silicon photovoltaic panels, J. Clean. Prod. 434 (2024) 140320, https://doi.org/10.1016/j.jclepro.2023.140320.
[114] C.C. Faircloth, K.H. Wagner, K.E. Woodward, P. Rakkwamsuk, S.H. Gheewala, The environmental and economic impacts of photovoltaic waste management in Thailand, Resour. Conserv. Recycl. 143 (2019) 260–272, https://doi.org/10.1016/j.resconrec.2019.01.008.
[115] S. Mahmoudi, N. Huda, M. Behnia, Environmental impacts and economic feasibility of end of life photovoltaic panels in Australia: a comprehensive assessment, J. Clean. Prod. 260 (2020) 120996, https://doi.org/10.1016/j.jclepro.2020.120996.
[116] H. Chowdhury, N.L. Chang, S. Song, Z. Xie, J. Zuo, Y. Shen, Life cycle assessment and techno-economic analysis of a laser-based end-of-life solar panel recycling process, Sol. Energy Mater. Sol. Cell. 302 (2026) 114358, https://doi.org/10.1016/j.solmat.2026.114358.
[117] G. Ansanelli, G. Fiorentino, M. Tammaro, A. Zucaro, A life cycle assessment of a recovery process from end-of-life photovoltaic panels, Appl. Energy 290 (2021) 116727, https://doi.org/10.1016/j.apenergy.2021.116727.
[118] R. Contreras Lisperguer, E. Muñoz Cerón, J. de la Casa Higueras, R.D. Martín, Environmental impact assessment of crystalline solar photovoltaic panels' end-of-life phase: open and closed-loop material flow scenarios, Sustain. Prod. Consum. 23 (2020) 157–173, https://doi.org/10.1016/j.spc.2020.05.008.
[119] F. Del Pero, M. Delogu, L. Berzi, M. Escamilla, Innovative device for mechanical treatment of end of life photovoltaic panels: technical and environmental analysis, Waste Manag. 95 (2019) 535–548, https://doi.org/10.1016/j.wasman.2019.06.037.
[120] J. Li, J. Shao, X. Yao, J. Li, Life cycle analysis of the economic costs and environmental benefits of photovoltaic module waste recycling in China, Resour. Conserv. Recycl. 196 (2023) 107027, https://doi.org/10.1016/j.resconrec.2023.107027.
[121] Q. Guo, C. Kluse, A framework of photovoltaics recycling facility location optimization, Sustain. Prod. Consum. 23 (2020) 105–110, https://doi.org/10.1016/j.spc.2020.04.003.
[122] F. Cucchiella, I. D'Adamo, P. Rosa, End-of-Life of used photovoltaic modules: a financial analysis, Renew. Sustain. Energy Rev. 47 (2015) 552–561, https://doi.org/10.1016/j.rser.2015.03.076.
[123] B. Crespo, C. Cavanaugh, A. Potter, S. Yaniger, G. Gaustad, C. Wilkinson, Technoeconomic feasibility of photovoltaic recycling, Int. J. Appl. Glass Sci. 15 (2024) 381–390, https://doi.org/10.1111/ijag.16679.
[124] I. D'Adamo, M. Miliacca, P. Rosa, Economic feasibility for recycling of waste crystalline silicon photovoltaic modules, Int. J. Photoenergy 2017 (2017) 1–6, https://doi.org/10.1155/2017/4184676.

[125] A. Rubino, G. Granata, E. Moscardini, L. Baldassari, P. Altimari, L. Toro, F. Pagnanelli, Development and Techno-Economic Analysis of an Advanced Recycling Process for Photovoltaic Panels Enabling Polymer Separation and Recovery of Ag and Si, Energies 13 (2020) 6690, https://doi.org/10.3390/en13246690.

[126] J.-K. Choi, V. Fthenakis, Crystalline silicon photovoltaic recycling planning: macro and micro perspectives, J. Clean. Prod. 66 (2014) 443–449, https://doi.org/10.1016/j.jclepro.2013.11.022.

[127] E. Markert, I. Celik, D. Apul, Private and externality costs and benefits of recycling crystalline silicon (c-Si) photovoltaic panels, Energies 13 (2020), https://doi.org/10.3390/en13143650.

[128] B. Hallam, M. Kim, Y. Zhang, L. Wang, A. Lennon, P. Verlinden, P.P. Altermatt, P. R. Dias, The silver learning curve for photovoltaics and projected silver demand for net-zero emissions by 2050, Prog. Photovoltaics Res. Appl. 31 (2023) 598–606, https://doi.org/10.1002/pip.3661.

[129] I. Celik, M. Lunardi, A. Frederickson, R. Corkish, Sustainable end of life management of crystalline silicon and thin film solar photovoltaic waste: the impact of transportation, Appl. Sci. 10 (2020) 5465, https://doi.org/10.3390/app10165465.

[130] Z. Ngagoum Ndalloka, H. Vijayakumar Nair, S. Alpert, C. Schmid, Solar photovoltaic recycling strategies, Sol. Energy 270 (2024) 112379, https://doi.org/10.1016/j.solener.2024.112379.